

Durability Properties of Nanomodified FRP-Concrete Adhesive Joints

A Thesis

Presented to the

Graduate Faculty of the

University of Louisiana at Lafayette

In Partial Fulfilment of the

Requirements for the Degree

Master of Science

Syed Ahnaf Morshed

Summer 2018

ProQuest Number:10844250

All rights reserved

INFORMATION TO ALL USERS

The quality of this reproduction is dependent upon the quality of the copy submitted.

In the unlikely event that the author did not send a complete manuscript and there are missing pages, these will be noted. Also, if material had to be removed, a note will indicate the deletion.



ProQuest 10844250

Published by ProQuest LLC (2019). Copyright of the Dissertation is held by the Author.

All rights reserved.

This work is protected against unauthorized copying under Title 17, United States Code
Microform Edition © ProQuest LLC.

ProQuest LLC.
789 East Eisenhower Parkway
P.O. Box 1346
Ann Arbor, MI 48106 – 1346

© Syed Ahnaf Morshed

2018

All Rights Reserved

Durability Properties of Nanommodified FRP-Concrete Adhesive Joints

Syed Ahnaf Morshed

APPROVED:

Jovan Tatar, Chair
Assistant Professor of Civil Engineering

Kenneth McManis
Professor of Civil Engineering

Qian Zhang
Assistant Professor of Civil Engineering

Vijaya K.A. Gopu
Professor of Civil Engineering

Mary Farmer-Kaiser
Dean of the Graduate School

Acknowledgments

First and foremost, I would like to thank my supervisor, Dr. Jovan Tatar, for his guidance, encouragement, and vital feedback in conducting and completing this thesis. I am also grateful to my other committee members, Dr. Kenneth McManis, Dr. Vijay Gopu and Dr. Qian Zhang, for their support. I would like to express my gratitude to my colleagues, Kamal Baral, Arkabrata Sinha, Shagata Das, and Tyler Young for all the knowledgeable discussions we have held during the course of this work. I would also like to thank Mark Le Blanc and my friend Salman Sakib for their assistance throughout my time in the University of Louisiana, Lafayette. I want to acknowledge the Graduate School and Department of Civil Engineering for supporting my graduate studies

I am very grateful to my parents: Kamrun Nahar and Dr. Syed Morshed Moula, and my sisters Nawmee and Nisha for their unwavering love and support. I am very thankful to my cousins Nahid Rahman, Nushrat Rahman, Muhib Noor Rahman, aunt Prof. Nurun Nahar Rahman, and beloved late uncle Prof. Mustafizur Rahman for always being there for me throughout my academic career.

Table of Contents

Acknowledgments	iv
List of Tables	vii
List of Figures.....	viii
1 Introduction	1
1.1 Goals and Objectives	2
1.2 Thesis Outline	3
2 Literature Review	4
2.1 Epoxy Adhesives	7
2.1.1 Incomplete cure.	8
2.1.2 Swelling and plasticization	10
2.1.3 Epoxy-cement paste interaction	12
2.2 Adhesive Bond Degradation Mechanisms	13
2.3 Nanoparticles	14
2.3.1 Nanosilica	16
2.3.2 Core-shell rubber.	18
2.3.3 Multi-walled carbon nanotubes (MWCNT).	21
2.4 Summary	23
3 Materials and Methods	26
3.1 Materials	29
3.1.1 Epoxy adhesives	29
3.1.2 Concrete.	30
3.2 Specimen Preparation	34
3.2.1 Epoxy dogbone specimens.	34
3.2.2 Differential scanning calorimetry (DSC).	38
3.2.3 CFRP-reinforced beam specimens for bond performance characterization.	39
3.3 Experimental Procedures	42
3.3.1 Moisture ingress.	43
3.3.2 Differential scanning calorimetry (DSC).	43
3.3.3 Tensile tests.	43
3.3.4 Three-point bending beam bond tests.	44
4 Results and Discussion	46
4.1 Moisture Ingress	46
4.2 Glass Transition Temperature (Tg)	47
4.3 Tensile Properties of Epoxy	49
4.3.1 Strength.	51
4.3.2 Elongation.	52
4.3.3 Modulus of elasticity.	53
4.4 Three-point Bending Beam Bond Test Results	54

4.5	Failure Mode of CFRP-Concrete Adhesive Joints	58
5	Summary and Conclusions	62
6	Future Work	66
7	References	68
	Abstract.....	74
	Biographical Sketch	76

List of Tables

Table 1: Mechanical properties of SMNS modified epoxy nanocomposite [37-42].	17
Table 2: Mechanical properties of CSR modified epoxy nanocomposite [46-52].	20
Table 3: Mechanical Properties of MWCNT incorporated epoxy composite[35, 53-59].....	22
Table 4: Test matrix	27
Table 5: Physical properties of the epoxy adhesives.....	29
Table 6: The mixing ratio of the resin and masterbatch.....	30
Table 7: Mix proportion of 10,000 psi small beam specimens	32
Table 8: Average compressive strength of cylinders for design 10,000 psi strength.....	33
Table 9: Step by step preparation of epoxy adhesives	35
Table 10: Failure mode of Control and ACP beam specimens	59

List of Figures

Figure 2.1: Loading modes in interfacial region [1].....	4
Figure 2.2: Three layered system consisting of concrete, epoxy, and FRP [14].	5
Figure 2.3: Example of failure mode transition from cohesive (dry condition) to adhesive (wet condition) with exposure to moisture [17].....	6
Figure 2.4: Failure mode of epoxy-concrete bond: (a) in dry ambient conditions; (b) in exposed conditions to moisture.....	6
Figure 2.5: Epoxide (pointed by arrow) group in a Diglycidyl ether of bisphenol-A molecule.....	7
Figure 2.6: Primary amine-epoxy reaction	8
Figure 2.7: Endothermic area in DSC curve [29]	9
Figure 2.8: Schematic representation of interphase region [31].....	13
Figure 2.9: Supposed structure of epoxy-rich region within interphase [31].	13
Figure 2.10: Scanning electron microscope (SEM) image of surface modified nano-silica [37].....	16
Figure 2.11: Structure of a core-shelled rubber, [Kaneka MX-960 datasheet].....	19
Figure 2.12: Atomic arrangement of CNT [12]	21
Figure 2.13: SWCNT and MWCNT, [35]	21
Figure 3.1: Dogbone specimen (type V).....	34
Figure 3.2: Epoxy injected into rubber mold	34
Figure 3.3: Dispersion of MWCNT based masterbatch epoxy by sonication	38
Figure 3.4: Portable concrete mixer.....	39
Figure 3.5: Aluminum-ply beam forms	40
Figure 3.6: Insertion of notch in the midspan of the small beam specimen	41
Figure 3.7: Needle scaling gun	42
Figure 3.8: Insertion of CFRP on the tension surface of the beam specimens by wet layup process.....	42

Figure 3.9: (a)Tensile test of dogbone specimen in mts; (b) Speckle pattern on a typical epoxy dogbone specimen.....	44
Figure 3.10: Three-point bending test setup; (a) Small beam specimen specification; (b) Three-point bending test fixtures of notched beam specimens.....	45
Figure 4.1: Moisture ingress of the epoxy adhesives.....	46
Figure 4.2: (a) Average Tg values of different sample; (b) Typical DSC curve of neat epoxy.....	49
Figure 4.3: Enthalpy relaxation.....	49
Figure 4.4: Typical stress vs strain curve of dogbone samples in control condition	50
Figure 4.5: Typical stress vs strain curve of dogbone samples in ACP.....	50
Figure 4.6: Strength of dogbone specimens in control and ACP.....	52
Figure 4.7: Elongation of dogbone specimens in control and ACP.....	53
Figure 4.8: Modulus of elasticity of dogbone specimens in control and ACP	54
Figure 4.9: Load vs displacement curve for control specimens.....	55
Figure 4.10: Load vs displacement curve for ACP specimens	55
Figure 4.11: Strength of control and conditioned small beam specimens	57
Figure 4.12: Bond strength retention	58

1 Introduction

Application of fiber-reinforced polymer (FRP) composites is an emergent novel technique in civil infrastructures. Typical FRP composite materials are comprised of fibers, such as glass or carbon, embedded in a polymer matrix. The fibers act as the primary reinforcement, while the polymer matrix (e.g., epoxy resin) acts as a binder, protecting the fibers by encapsulating them, and transferring stress between the fibers. Applications of FRP in structural engineering includes reinforcing bars, column confinement with externally bonded FRP wraps, composite jackets, prefabricated pultruded rods or plates etc.[1].

FRP composites can be formed on-site utilizing the wet lay-up process in which a dry fiber fabric, is impregnated with epoxy and directly bonded to a prepared concrete substrate. Following application, the impregnating epoxy cures in ambient conditions to form a composite. The externally bonded FRP acts as a supplemental reinforcement that can improve structural members' strength and stiffness [2-6].

Epoxy resin is the most common adhesive used in externally bonded FRP-concrete substrate. Effective bonding between FRP and concrete substrate depends on the mechanical interlock and chemical bonding between the adhesive and the substrate. The purpose of the adhesive bond between epoxy and concrete is to sustain the forces in interfacial region when load is applied, so that force transfer between the structural member and externally bonded FRP can be accomplished [7]. However, even when the bond conditions are ideal, the full tensile capacity of externally bonded FRP often cannot be fully utilized due to relatively very low strength of the concrete substrate. As a result, debonding failure of FRP occurs [8-9].

Externally bonded FRP systems prone to debonding exhibit further loss in strength when exposed to continued moisture cycles which lead to loss of adhesion [10]. Prior research has

also shown that this loss of adhesion is due to complex competing degradation mechanisms at the epoxy-concrete interfaces [11]. There is some evidence that indicates that the decay in epoxy adhesives' mechanical properties when exposed to moisture can be remedied by addition of nanoparticles to the adhesive [12,13]. The main objective of this study is to understand if nanomodified epoxy adhesives can improve the durability of the adhesive joint between externally bonded FRP and concrete when subjected to a hygrothermal accelerated conditioning protocol. Prior to this study, insignificant research has been performed to determine the effects of epoxy modified with various nanoparticles on the strength and durability of externally bonded FRP-concrete adhesively bonded joints.

1.1 Goals and Objectives

The principal objective of this study is to elucidate the effects of Bisphenol A-based epoxy modified with commercial surface-modified nano-silica, core-shell rubber (CSR), and multi-walled carbon nanotubes (MWCNT) nanoparticles *on the strength and the durability of FRP-concrete adhesively bonded joints*. The objective of this research will be accomplished by performing the following tasks:

Task 1: Perform moisture ingress tests on neat and nanomodified epoxies to understand the absorption capacity of the epoxy for moisture.

Task 2: Perform Differential Scanning Calorimetry test on nanomodified epoxy adhesives under control and accelerated conditioning protocol (ACP) environments to identify the effects of ACP on glass transition temperature and enthalpy relaxation.

Task 3: Perform tensile tests on epoxy dogbone specimens to evaluate the effect of nanoparticle addition on epoxy's mechanical properties and durability.

Task 4: Perform three-point bending test on beams reinforced with FRP to determine the effect of nanoparticle addition to epoxy on FRP-concrete bond strength and durability.

1.2 Thesis Outline

Chapter 1 discusses the importance of using Fiber Reinforced Polymer (FRP) composite in structural engineering and lays out the motivation, and goals and objectives for the study.

Goals and objectives of this research are also highlighted at the end of the chapter. Chapter 2 presents background information on: (a) the effect of aggressive environmental conditions on epoxy; (b) degradation mechanisms in externally bonded FRP-concrete joints; and (c)

nanomodified epoxy adhesives. Chapter 3 provides a brief information about the test matrix and the properties of the materials used in this research. It also includes information about materials specification and specimen preparation procedures. Additionally, this chapter highlights the methodology and the experimental procedures of the research study.

Experimental results and discussions on tensile test, differential scanning calorimetry (DSC), three-point bending test are presented in Chapter 4. Summary and conclusion are provided in Chapter 5. Finally, the future work is discussed in chapter 6.

2 Literature Review

Typical externally bonded FRP-repairs fail by debonding. At the structural scale, the externally bonded FRP can be subjected to Mode I, Mode II or Mixed Mode loading condition as shown in Figure 2.1. Mode I loading condition (or pure tension) is typical for the ends of the bonded laminates. Mode I loading condition causes peel failure mode which starts at the ends of the laminates and propagates towards the midspan [14]. Mode II (or pure shear) loading condition is observed in the vicinity of vertical flexural cracks. When concrete's tensile capacity is reached, flexural cracks are initiated; and as a result, FRP is loaded in direct shear [14]. Mixed Mode loading condition is typical for FRP composite near shear-flexure cracks [14]. Mode I and Mixed Mode failure can be prevented by providing appropriate anchorage. Thus, debonding caused by the Mode II loading condition usually governs the failure of externally bonded FRP repairs in flexural members.

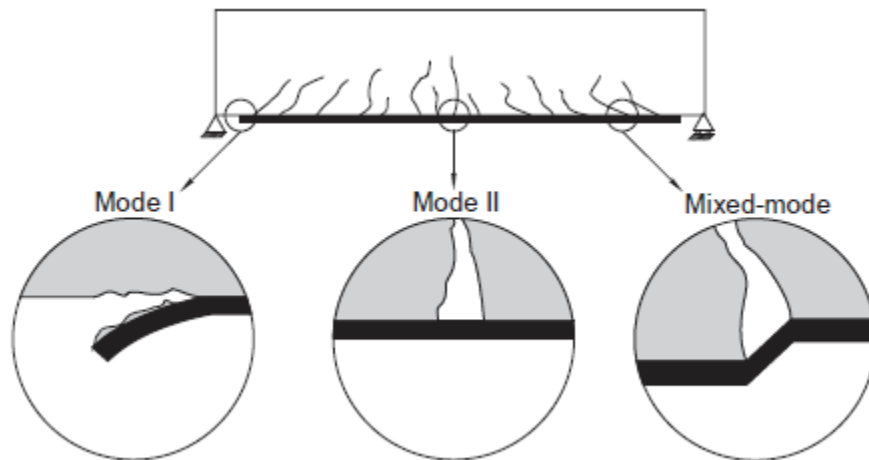


Figure 2.1: Loading modes in interfacial region [1]

Externally bonded FRP is applied to concrete structures via epoxy adhesives that are cured in ambient conditions. Epoxy acts as a medium between the FRP and concrete and is

responsible for transfer of stress between the adherents. Integrity of the adhesive bond governs the performance of an externally bonded FRP repair.

There are five possible failure modes in externally bonded FRP systems (Figure 2.2). Out of five, first four can be considered debonding failure modes: (a) failure along the interface between concrete and adhesive (also known as adhesive failure mode); (b) failure within the concrete substrate (also known as cohesive failure mode); (c) failure along the interface between FRP and adhesive; and (d) failure of the adhesive and (e) FRP rupture. Cohesive failure mode (failure within the concrete substrate) is the most desirable debonding failure mode as it indicates good adhesion between the adherents. Under moisture ingress, the failure mode shifts from cohesive to a less desirable adhesive failure mode (interfacial separation between the adhesive and substrate) (Figure 2.3) [15]. Failure modes corresponding to adhesive decohesion and interfacial failure between FRP and the adhesive rarely occurs. FRP rupture is also infrequent and occurs when the members are under-reinforced, exposed to aggressive environments that deteriorate the FRP composite, or when high interlaminar stresses are developed [16].

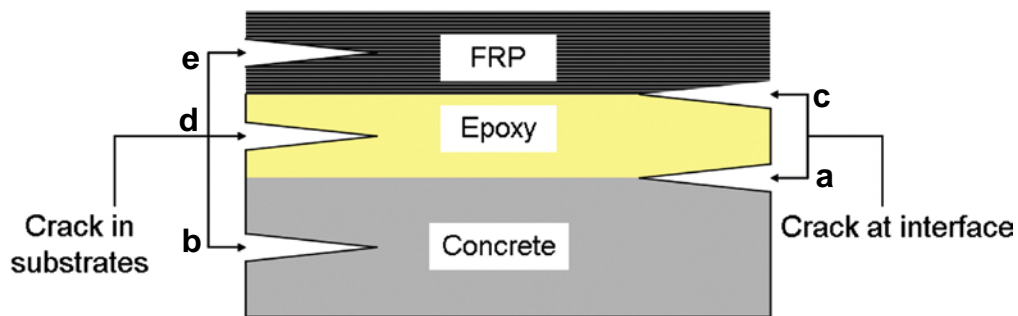


Figure 2.2: Three layered system consisting of concrete, epoxy, and FRP [14].

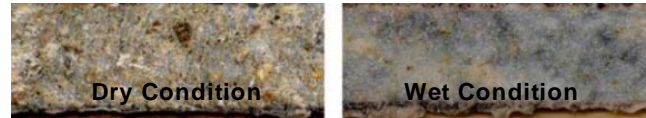


Figure 2.3: Example of failure mode transition from cohesive (dry condition) to adhesive (wet condition) with exposure to moisture [17].

At macroscopic level, the adhesive bond between externally bonded fiber reinforced polymer (FRP) and concrete is formed through a combination of mechanical interlocking and chemical bonding (Figure 2.4). The nature of the chemical bond formed at the surface level between epoxy and cement paste is mostly hydrogen bonding; these bonds are weak and susceptible to deterioration under moisture ingress [17]. As the epoxy penetrates into the pores and crevices of the roughened surface of the concrete substrate, a mechanical interlock with the substrate is formed. The integrity of mechanical interlock can be compromised when stiffness of the epoxy adhesive is reduced, which can occur with moisture ingress and at ambient temperatures higher than glass transition temperature (T_g) of epoxy as it will be explained in Section 2.2.

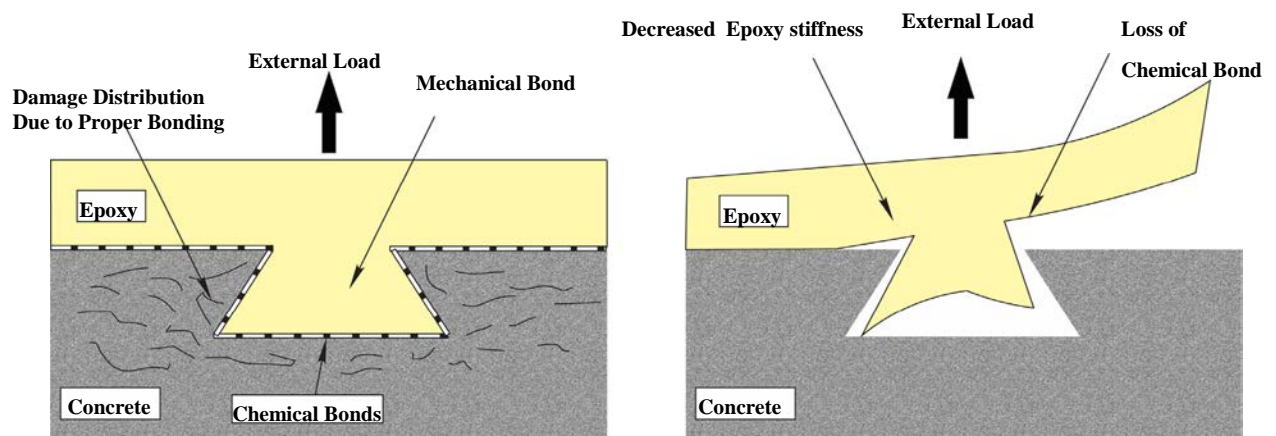


Figure 2.4: Failure mode of epoxy-concrete bond: (a) in dry ambient conditions; (b) in exposed conditions to moisture

2.1 Epoxy Adhesives

Epoxy resins are widely used as adhesives, protective coatings and as matrix in fiber reinforced polymer (FRP) composites. Diglycidyl ether of bisphenol A (DGEBA) epoxy resin is one of the most commonly and extensively used structural epoxy adhesives (Figure 2.5) The term “epoxy” originates from the chemical composition of the molecule comprising of an oxygen atom bound to two linked carbon atoms. The term is commonly applied to a three-component ring called oxirane or epoxide.

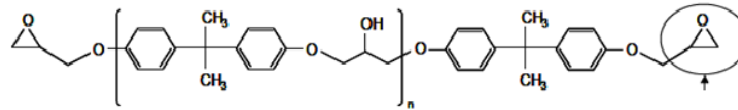


Figure 2.5: Epoxide (pointed by arrow) group in a Diglycidyl ether of bisphenol-A molecule.

The epoxy molecule reacts with a curing agent (hardener) to form a rigid cross-linked network (Figure 2.6). Most common types of hardeners are amines. Amine compounds in the hardener are categorized into primary, secondary, and tertiary amines, in which one, two, and three molecule(s) of ammonia (NH_3) have been substituted for hydrogen, respectively. Addition of a hardener containing hydrogen atoms to epoxy opens the three-membered epoxide ring resulting in the formation of a hydroxyl (OH^-) group. In the ring opening reaction, the active epoxide groups react with a hardener to form permanent covalent bonds (cross-links) between the epoxy polymeric chains resulting in highly cross-linked, three-dimensional structure [18]. In cross-linking of an epoxy resin with an amine hardener, the epoxy group reacts with the primary amine.

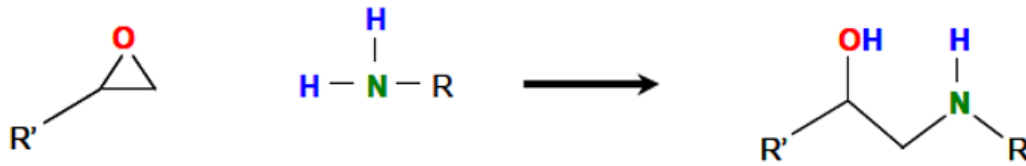


Figure 2.6: Primary amine-epoxy reaction

2.1.1 Incomplete cure. At the completion of curing, cross-linking process stops and epoxy is considered to have developed its full mechanical properties [19]. However, full cure is possible only under controlled curing conditions (e.g., staged cure), but not in ambient environments characteristic for infrastructure applications [20]. As a result, incomplete cross-linking takes place which renders epoxy adhesives more vulnerable to the environmental loadings [21]. The degree of cure of epoxy that is achieved at ambient temperature is deemed suitable for structural applications [22]. The “cold-curing” process, however, may limit the adhesive’s durability.

With increasing temperature, amorphous polymers such as epoxy experience a glass transition rather than a melting point, which involves neither an endothermic nor an exothermic process. The physical transition from a glassy state to a rubbery state is defined by a glass transition temperature (T_g). T_g is identified solely by a change in specific heat capacity. Differential Scanning Calorimetry (DSC) is one of the most commonly used methods to detect changes in heat capacity and endothermic/exothermic processes in epoxy adhesives by measuring the rate of heat transfer (heat flux). Glass transition is characterized by a step change in the DSC curve baseline. A constant heat flow difference is observed in the DSC curve before the glass transition occurs. However, immediately after glass transition, there is an increase in the heat flow difference. The increase in heat flow

difference is proportional to the increase of specific heat capacity. This phenomenon occurs when an epoxy transitions from glassy state to rubbery state. Epoxy when subjected to DSC testing, experienced an endothermic area (Figure 2.7). This area appeared in conjunction with the glass transition step change. This area is the result of enthalpy relaxation as the temperature of the epoxy increases. Initially, in cured epoxy potential energy is restored internally. As the glass transition temperature is approached and epoxy is about to transition into a rubbery state an endothermic curve appeared. As a result, heat is absorbed by the epoxy matrix to release the restored internal forces resulting in an endothermic curve.

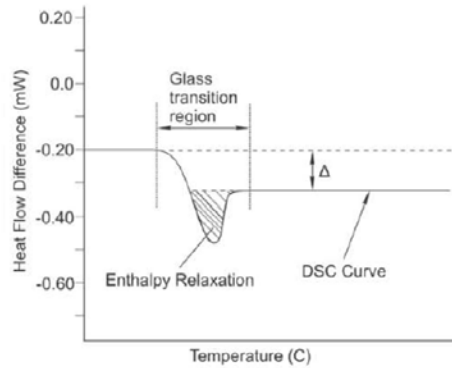


Figure 2.7: Endothermic area in DSC curve [29]

Temperature increase has a significant effect on the mechanical properties of epoxy. At a temperature lower than the T_g , i.e. in the glassy (brittle) state, chain mobility of the cross-linked network is restricted, but as the temperature exceeds T_g , chain mobility of the cross-linked chains increases. When the service temperature exceeds T_g of the epoxy, mechanical properties of the epoxy are affected. Increased chain mobility leads to degradation of strength and elastic modulus, while the ductility and fracture toughness are usually improved. Higher cross-linking density, characteristic of fully cured epoxy, yields higher T_g when compared to epoxies cured under ambient conditions. This often poses a risk for the integrity of external

FRP repairs, as the typical T_g of ambient-cured epoxies within the range of 45°C to 60°C, which can be exceeded in many warmer climates. For comparison, fully cured resins can achieve T_g between 65°C and 105°C, which is above the maximum design temperature for most infrastructure applications [23].

2.1.2 Swelling and plasticization. Exposure of epoxy to moisture degrades its mechanical and thermal properties: (a) plasticization of the epoxy matrix (caused by moisture ingress) reduces stiffness of the epoxy; and (b) weak hydrogen bonds can be disrupted by water molecules along the epoxy-concrete interface leading to loss of adhesion [18,24].

On a microscopic level, voids are present within the polymeric chain network of the epoxy. These voids are due to the atomic packing irregularities and are usually referred to as a *free volume* [25]. As epoxy curing reaction results in the formation of hydroxyl groups in the network, water molecules are attracted to the cross-linked network through the interaction with the polar hydroxyl group via hydrogen bonding [26,27]. The water molecules bonded to the polymer network via hydrogen bonding generate additional space between cross-linked polymer chains, thereby enlarging the free volume and causing hygroscopic swelling. The swelling of the adhesive is deemed partially responsible for the loss in adhesive bonding properties. As adhesive swelling is constrained by the rigid adherents (in case of this study FRP and concrete substrate), interfacial residual stresses are generated.

With an increase in free volume, chain mobility increases due to the availability of space within the polymeric chain network. Consequently, less thermal energy is required to convert epoxy into rubbery state i.e. lower T_g is experienced. At this stage, epoxy loses its stiffness. This process is referred to as *plasticization*, which renders water – a *plasticizer*. Plasticization of epoxy involves: (a) lowering of rigidity at room temperature; (b) lowering of temperature

at which substantial deformations can be affected with not too large forces; (c) increase of the elongation to break at room temperature; and (d) increase of the toughness (impact strength) down to the lowest temperature of serviceability [28]. Plasticization occurs by replacement of inter-chain interactions by the plasticizer molecules, in this case water. Plasticization has a significant effect on the chain mobility in low cross-linked network. However, higher cross-linked density of epoxy resists opportunities for unreacted functional group to interact with water molecules which diminishes the effects of plasticization [28].

Sub- T_g thermal aging process (or post-cure) of polymeric structure induces densification of the molecular structure. As a result, a rigid molecular structure characteristic of high cross-link density is formed. There are two changes that occur to the molecular structure of an epoxy during post-cure: (a) reduction in free volume and (b) restriction in chain mobility within the molecular network. Reduction in free volume during the post-cure, diminishes the total amount of volume in the polymeric network in which water transportation occurs due to moisture ingress. As the free volume decreases, the capacity of the epoxy to hold moisture decreases. Post-cure and moisture ingress influence each other in the following way.

Absorbed water reduces interchain physical interaction by forming breaking interactions between the polymer chains. Thus, plasticization occurs in the polymeric network. Increased chain mobility due to plasticization effect can then facilitate the post-cure process and free volume is reduced.

Enthalpy relaxation represents the amount of heat energy necessary to remobilize the polymeric chain [29]. Initially, at the beginning of the cure process, when T_g is below the curing temperature, enthalpy relaxation is large. Uncured epoxy can have a relatively high amount of free volume (low cross-linking density), which results in a high enthalpy

relaxation. With the ongoing curing process, the free volume decreases (high cross-linking density) and, as a result, the enthalpy relaxation diminishes [29,30]. Hence, with post-cure T_g gradually increases while the enthalpy relaxation diminishes.

2.1.3 Epoxy-cement paste interaction. The plane of contact between the epoxy surface and the surface of the cement paste is called the *interface*. From a macroscale point of view, the interface divides the two adherents. Even though “interface” may be apparent at the larger length scales, recent research [31] showed evidence that a transition region called *interphase* exists between bulk epoxy and bulk cement paste substrate. The presence of this region is caused by permeation of low-viscosity epoxy into the porous network of a cementitious material substrate, as well as the preferential reaction between amine-based hardener and cement hydrates. This preferential reaction is deemed to cause shortage of amines adjacent to the interface (as shown in Figure 2.7) [31]. As a result, it is thought that epoxy adjacent to plane of contact between epoxy and substrate is characterized with lower cross-linking density than the bulk epoxy. This epoxide-rich region (lower degree of cure) is hypothesized to be adjacent to the amine-rich region as shown in the Figure 2.8. The presence of epoxide-rich region is deemed to render the interface more vulnerable to environmental degradation [32].

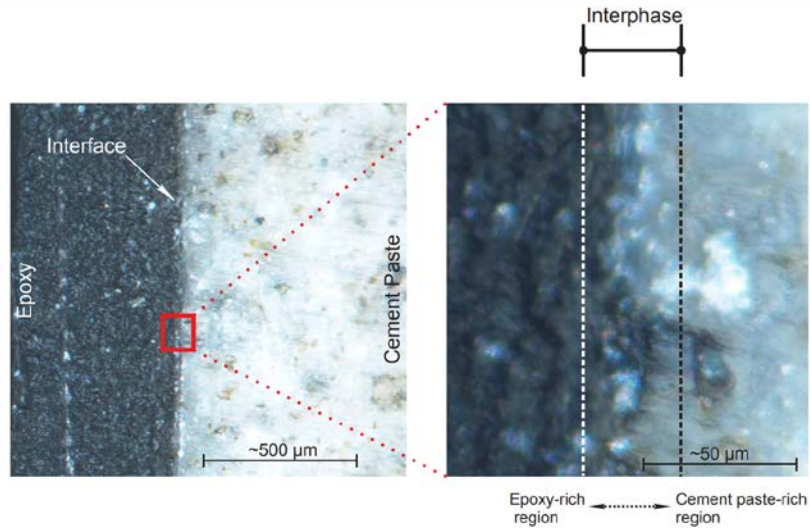


Figure 2.8. Schematic representation of interphase region [31]

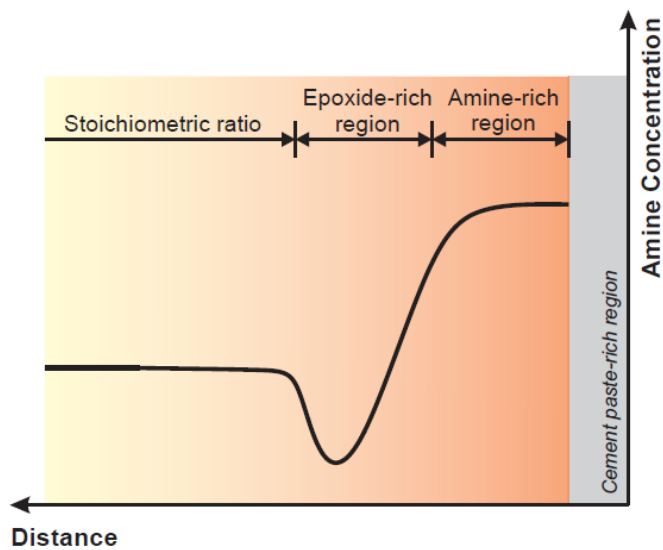


Figure 2.9: Supposed structure of epoxy-rich region within interphase [31].

2.2 Adhesive Bond Degradation Mechanisms

Exposure to moisture was found to be the most critical factor in the adhesive bond degradation. As per the literature review, moisture-driven adhesive bond degradation is thought to occur through a synergistic effect of the following mechanisms [33-35]:

- (a) Moisture ingress leads to swelling of adhesive inducing a residual interfacial stress.

(b) Stiffness of the adhesive decreases due to plasticization effect of water on the cross-linked network of the epoxy adhesive which disrupts the integrity of the mechanical interlock between the adherents.

(c) Moisture ingress increases polymeric chain mobility which in turns reduces the T_g . In warm climates, due to the moisture ingress-driven reduction in T_g integrity of the adhesive bond may be compromised.

(d) Intermolecular hydrogen bonds formed between epoxy and concrete along the interface are disturbed due to moisture ingress.

(e) Presence of epoxide-rich region (lower cure than bulk epoxy) adjacent to the adhesive-substrate interface could lead to increased vulnerability of the interface to moisture-driven degradation.

2.3 Nanoparticles

At ambient temperature in the field conditions, epoxy does not fully cure. As a result, incomplete cross-linking takes place which prevents epoxy from developing its full mechanical properties. In this work, addition of nanoparticles is explored as a means of offsetting some of the deficiencies of ambient-cured epoxy over fully cured epoxy.

Nanoparticles deemed suitable for structural applications are selected to maintain low viscosity of the adhesive while maximizing mechanical property enhancement, considering the following characteristics: (a) small particle size; (b) high content of reactive functional group to ensure compatibility between the resin and nanoparticle; and (c) uniform dispersion ability. As pointed out by numerous researchers, added nanoparticles may develop attractive forces with polymers such as epoxy [35]. Nanoparticles' superior mechanical properties

combined with attractive nanoparticle-matrix interactions can likely facilitate cross-linking and enable the nanocomposite to develop mechanical properties superior to those of neat epoxy.

It is assumed the addition of nanoparticles as an additional phase in epoxy, may diminish free volume and resist chain mobility within the epoxy polymer chain network. As a result, the effect of plasticization can be potentially reduced. In the field conditions, if degradation of stiffness is avoided – then improvement in the mechanical interlock between adherents can be achieved. Additionally, functional reactive groups of nanoparticles are deemed able to react with unreacted epoxide-groups within the interphase region, thus helping expedite cross-linking and improving mechanical properties of the interphase.

As previously discussed, many studies have shown that T_g and mechanical properties of epoxy depend upon curing temperature and duration [36]. Ideally, mechanical properties such as stiffness and strength tend to increase with the cross-linking process. However, previous work has established that epoxies having high cross-link density possess inherently low fracture toughness, so there is usually a tradeoff between high strength and stiffness, and fracture toughness. Homogenously dispersed nanoparticles in the epoxy resin can act as a medium that improves fracture toughness of the epoxy and interface, while maintaining high strength and stiffness of the adhesive [36,37].

Extensive studies have been performed on improvements of mechanical properties of epoxy through addition of nanoparticles [36,37]. However, the adhesion properties of epoxy nanocomposites and their potential to offset degradation in the adhesive joints have been subjected to very little research. In this study, potential of nanocomposites as adhesives in the infrastructure and their mechanical property-improving effect on bond durability have been

explored. Three of the most commonly studied types of nanoparticles were evaluated in this work: nanosilica, elastomers and rubber particles, and carbon nanotubes.

2.3.1 Nanosilica. Silicon dioxide nanoparticles, also known as silica nanoparticles or nanosilica is a commonly used second phase in epoxy. Nanosilica is produced by sol-gel process which involves conversion of monomers into a colloidal solution (*sol*) that acts as the precursor for an integrated network (or *gel*) of either discrete particles or network polymers [37].

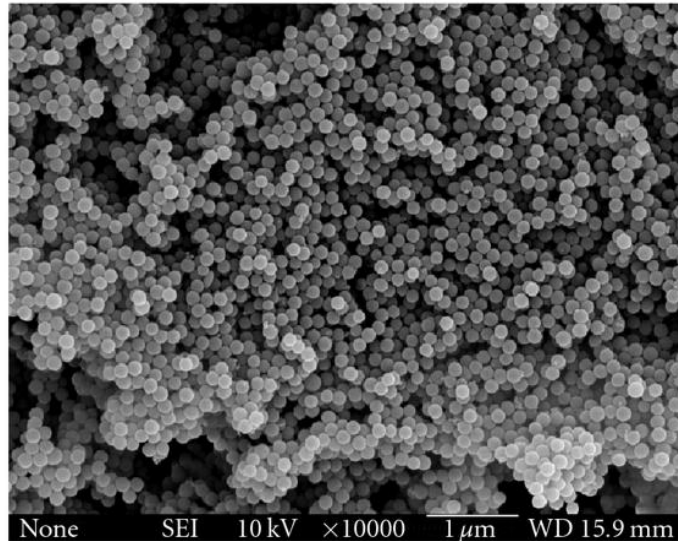


Figure 2.10: Scanning electron microscope (SEM) image of surface modified nano-silica [37]

Epoxy doped with surface modified nanosilica demonstrates enhanced elastic modulus, yield strength and fracture toughness over the neat epoxy [37]. The mechanical-property-enhancing effects from different studies are summarized in Table 1. Loading ratio between (0.1~10 wt%) of surface modified silica nanoparticles in epoxy resin can increase fracture toughness by up to 55% in comparison with the neat epoxy. However, at loading ratio greater than 10%, fracture toughness of the nanocomposites increased by 175% Research also

showed that nanosilica nanocomposite with loadings greater than or equal to 10 wt% increased elastic modulus (E) by up to 30% and ultimate tensile strength (UTS) by up to 10%. reported.[38-42].

Table 1: Mechanical properties of SMNS modified epoxy nanocomposite with percentage increase in parentheses [37-42].

Studies (Year)	Nanoparticle (Producer)	Resin	Particle Loading (wt %)	E (GPa)	UTS (MPa)	Fracture Toughness, G_{IC} (J.m ⁻²)
Chen et. al. (2012)	Nanopox E430	Epoxy (DGEBA+ proprietary hardener)	0.1	2.32 (5%)	-	400 (12%)
Blackman et. al. (2007)	Nanopox F400	Epoxy (DGEBA + proprietary hardener)	4.0	3.20 (8%)	-	132 (52%)
J. Ma et. al. (2008)	Nanopox F400	Epoxy (DGEBA + Jeffamine D230)	10.0	3.64 (32%)	58.3 (2.7%)	370 (105%)
J. Ma et. al. (2008)	Nanopox F400	Epoxy (DGEBA + 4,40-Diaminodiphenyl sulfone)	10.0	3.79 (16%)	104.3 (1.8%)	110 (63%)
Tang et. al. (2008)	Nanopox E470	Epoxy (DGEBA+ proprietary hardener)	10.0	3.79 (18%)	54 (22%)	291 (76%)
D. Bray et al (2013)	Silica SM ^h Organo-silicane	Epoxy (DER331+Piperidine) (DGEBA)	2.5	3.5 (0%)	83 (0%)	700 (125%)
J. Ma et. al. (2008)	Nanopox F400	Epoxy (DGEBA + Jeffamine D230)	20.0	3.85 (40%)	59.5. (4.2%)	660 (266%)

J. Ma et. al. (2008)	Nanopox F400	Epoxy (DGEBA + 4,4-Diaminodiphenyl sulfone)	20.0	4.48 (39%)	107.4 (22%)	130 (86%)
----------------------	--------------	---	------	------------	-------------	-----------

A study has been performed on applying nanomodified epoxy (SMNS+ DGEBA) as adhesives on concrete cylinder blocks and masonry blocks in accelerated environmental conditions (immersion under water at 50°C for 3 weeks). Nanomodified and neat epoxy adhesives were cured for 8 months before immersing in water for 3 weeks. DSC test result showed that the nanocomposite experienced a 16% increase in T_g over the neat epoxy after 8 months of cure. Test results showed that the bond strength due to application of the hybrid system improved by 62% over the control group (neat epoxy). However, the mechanical properties of both neat and hybrid adhesives degraded when immersed in water for 3 weeks. Flexural strength and modulus of the hybrid system decreased by 19% and 20% respectively whereas in case of neat epoxy the flexural strength and modulus were decreased by 31% and 29%. Improvement in adhesive joint strength of concrete with application of SMNS-modified epoxy in accelerated environmental conditions indicated promise for nanomodified epoxy to improve bond durability [43-45].

2.3.2 Core-shell rubber. Traditionally, addition of reactive liquid rubbers such as carboxyl-terminated butadiene acrylonitrile (CTBN) to epoxy results in enhancement of fracture toughness CTBN's are usually soluble in uncured epoxy. However, they tend to agglomerate during phase separation of fast cured epoxy, which leads to reduction in yield strength and stiffness. Another issue with CTBN based epoxy is that, the matrix is not applicable where low viscosity is required e.g. structural applications [46].

Core-shell rubber (CSR) consisting of a rubbery core and a thin-layered shell (Figure 2.10) is the second generation of rubber modifiers for epoxy. CSR replaced liquid rubbers as toughening agents as they provide better enhancements such as ductility and fracture toughness, while not significantly affecting strength and elastic modulus [46]. Unlike CTBN, the particle size and the volume fraction of the CSR as modifiers can be controlled. The presence of outer shell helps the inner rubber layer to retain its shape and size.

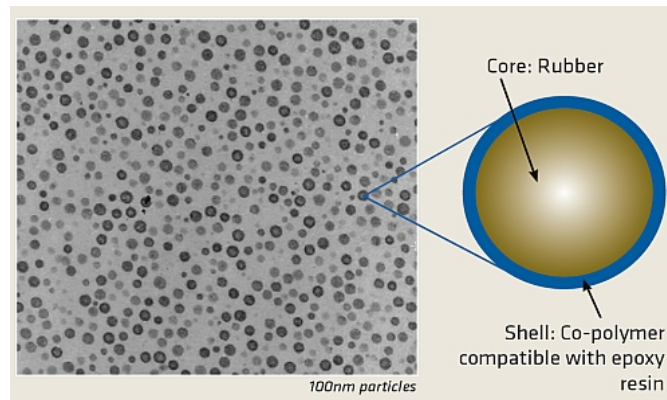


Figure 2.11: Structure of a core-shelled rubber, [Kaneka MX-960 datasheet]

The rubbery core of CSR is made of either acrylic or butadiene based rubbers which is generally not compatible with the base resin. The shell is designed based on the chemical structure of the epoxy resin and the desired interfacial properties, which makes the nanoparticle compatible with the base resin. Additionally, CSR-modified epoxy maintains low viscosity compared to CTBN-modified epoxy which makes handling and the curing process more convenient.

CSR-modified epoxy was reported to have improved fracture toughness over the neat epoxy. Fracture toughness of the CSR-toughened epoxy can be improved by up to 88% [46-51]. However, elastic modulus of CSR toughened epoxy systems was found to deteriorate by up to 23%. Additionally, lack of significant improvement in strength was observed. The

deterioration of strength in CSR-modified epoxy it thought to be due to the cavitation of the particles followed by void growth [52]. The mechanical-property-enhancing effects of CSR from different studies are summarized in Table 2

Table 2: Mechanical properties of CSR modified epoxy nanocomposite with percentage increase in parentheses [46-52].

Studies (Year)	Nanoparticle (Producer)	Resin	Particle Loading (wt %)	E (GPa)	Fracture Toughness, K_{IC} (Mpa.m ^{1/2})
Dong Quan et. al. (2015)	CSR (Manufacturer Unknown)	Epoxy (Araldite LY556+ Albidur HE 600)	9.0	2.21±.02 (-20%)	1.25±0.16 (145%)
Chen et. al. (2014)	Poly-siloxane CSR	Epoxy (Araldite LY556+ Albidur HE 600)	10.0	2.55±.06 (-20%)	1.31±.04 (88%)
Carolan et. al. (2016)	Polyhedral Oligomeric Silses-quioxane POSS- Rubber	Epoxy (DGEBA + Aromatic Diamine)	2.0	2.5±.01 (5%)	1.63±0.11 (30%)
Youngran Jo et al (2015)	Polybutadiene-graft-polystyrene (PB-g-PS)	Epoxy (DGEBA + methyl tetrahydro phthalic anhydride (MeTHPA))	7.5	14 Pa (Strength) 55%	(-)
Wang et al (2009)	EPON 862+ Epikure W	Kane Ace MX 130	5%	2.4 (-4%)	33 (Impact Resistance) (150%)

2.3.3 Multi-walled carbon nanotubes (MWCNT). Carbon nanotubes (CNTs) are made of cylindrical rolled up graphene (vapor grown) sheets and fullerene structure. CNT consists of three different types: (a) single-walled CNT (SWCNT), (b) double-walled CNT (DWCNT) and (c) multi-walled CNT (MWCNT). Their atomic arrangements can be categorized into three groups, namely zigzag (A), chiral (B) and armchair (C).

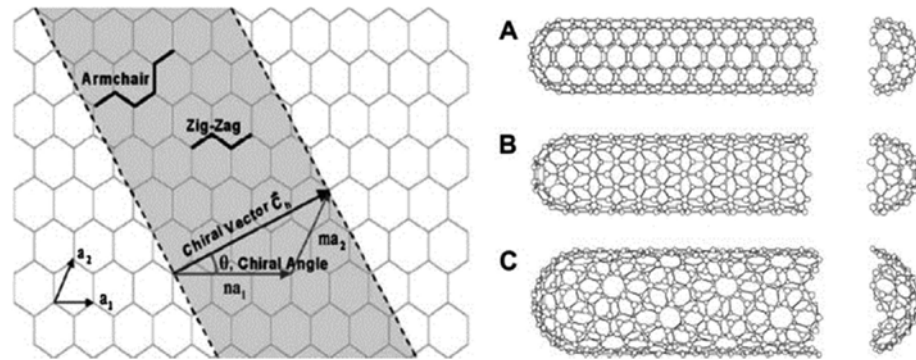


Figure 2.12: Atomic arrangement of CNT [12]

The major difference between single-walled carbon nanotube (SWCNT) and MWCNT is that SWCNT consists of a single graphene cylinder whereas MWCNT are comprised of several concentric graphene cylinders

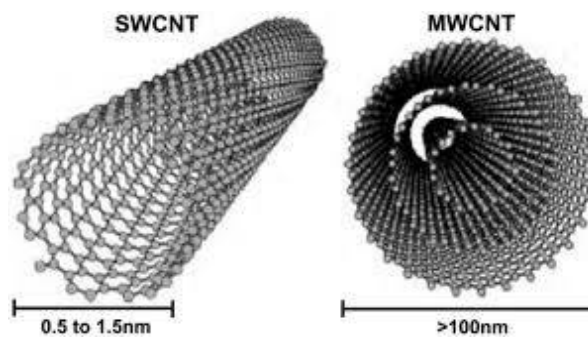


Figure 2.13: SWCNT and MWCNT, [35]

Higher loading of MWCNT in epoxy leads to the agglomeration in the epoxy matrix. Due to poor dispersion and weak bonding between the matrix and MWCNT, reduction in strength is

observed in the cured nanocomposites [37]. Furthermore, the epoxy modified with MWCNT was reported to suffer deterioration in strain at break and elastic modulus.

Factors such as (a) specific surface area (SSA), (b) preservation of a high aspect ratio and (c) homogeneous dispersion play a vital role in the improvement of mechanical properties of MWCNT nanocomposites. If sufficient surface area can be provided in MWCNT to facilitate the stress transfer between the matrix and MWCNT, uniform dispersion can be achieved. Additionally, due to presence of numerous layers with bigger diameters, MWCNTs enhance dispersibility compared to SWCNT in matrices such as epoxy.

Multiple studies point out that addition of MWCNT in epoxy can improve the adhesive's mechanical properties (Table 3). Fracture toughness (G_{IC}), ultimate tensile strength (UTS), elastic modulus (E) respectively increased by up to 54%, 5% and 16% at loading ratio 0.1 wt% compared to neat epoxy [53-59].

Table 3: Mechanical properties of MWCNT modified epoxy composite with percentage increase in parentheses [35, 53-59].

Studies (Year)	Nanoparticle (Producer)	Resin	Particle Loading (wt %)	E (GPa)	UTS (MPa)	Fracture Toughness G_{IC} ($J.m^{-2}$)
Ayatollahi et. al. (2011)	MWCNT (unknown)	Epoxy (ML-506)	0.1	3.24 (28%)	71.7 (5%)	1079 (29.5%)
Gojney et. al. (2005)	MWCNT (Elicarb)	Epoxy (DGEBA + H137i)	0.1	2.88 (29%)	64.7 (1.4%)	227 (39%)
G. Gkikas et. al. (2012)	MWCNT (Arkema)	Epoxy (Araldite LY 564)	0.5	2.50 (4%)	30 (25%)	390 (95%)

Karapappas et. al. (2009)	MWCNT (C 150P)	Epoxy (Bisphenol-A)	0.5	2.89 (0.4%)	72.2 (-1.7%)	110 (57%)
Tang et. al. (2013)	MWCNT (Time Stub)	Epoxy (DGEBA)	1.0	3.06 (4%)	73.5 (-4%)	140 (58%)
Hsieh et. al. (2011)	MWCNT (Produced)	Epoxy (DGEBA) LY-556	0.1	3.01 (4%)	(-)	162 (22%)
Hsieh et. al. (2011)	MWCNT (Produced)	Epoxy (DGEBA) LY-556	0.2	3.11 (7%)	(-)	188 (41%)
Hsieh et. al. (2011)	MWCNT (Produced)	Epoxy (DGEBA) LY-556	0.5	3.26 (12.5%)	(-)	223 (68%)
Tang et. al. (2011)	MWCNT (C150P)	Epoxy (DGEBA+ Albidur HE600)	0.5	2.89 (1%)	72.2 (-1.5%)	110 (72%)

2.4 Summary

External reinforcing or retrofitting by externally bonded FRP has become a popular method for ensuring longevity of older structures. Fiber-reinforced polymer (FRP) products, especially CFRP, are generally applied to structural members to enhance its strength and stiffness. CFRP laminates are externally bonded to the tension faces of the flexural elements using epoxy adhesives via dry or wet lay-up process.

Typical externally bonded FRP-repairs fail by debonding. Epoxy acts as a bonding medium between the FRP and concrete and is responsible for the transfer of stress between the

adherents. The performance of an externally bonded FRP repair is governed by the integrity of the adhesive bond. Ambient-cured epoxy adhesives generally used in externally bonded FRP-repairs do not achieve full cure in the field conditions, which renders them susceptible to environmental degradation.

At a microscopic level, the adhesive bond between externally bonded fiber reinforced polymer (FRP) and concrete is formed through a combination of mechanical interlocking and chemical bonding. Mechanical interlock between the substrate and the adherent forms as the adhesive penetrates into the pores, holes, and irregularities of the surface, and locks mechanically to the substrate. The integrity of mechanical interlock can be compromised when stiffness of the epoxy adhesive is reduced, which can occur with moisture ingress (also known as plasticization) and at ambient temperatures higher than glass transition temperature (T_g) of epoxy. The nature of the chemical bond formed at the surface level between epoxy and cement paste is mostly hydrogen bonding. Due to the polar nature of hydrogen bonds, the chemical bond is vulnerable to moisture ingress.

In addition, moisture ingress disrupts cross-linked polymer chains present in the epoxy. This enlarges the free volume and causes hygroscopic swelling of epoxy which can lead to development of residual stress along the bond-line. Moreover, interphase region which is adjacent to the plane of contact between epoxy and substrate is characterized with lower cross-linking density than the bulk epoxy. This region has lower degree of cure and is deemed more vulnerable to environmental degradation than bulk epoxy.

Addition of nanoparticles to neat epoxy is known to improve the properties of the base resin. It is thought that this mechanical-property-enhancing effect of nanoparticles may offset some of the deficiencies of ambient-cured epoxies, in particular when related to durability.

This work explored three of the most studied types of nanoparticles: (a) surface-modified nanosilica (SMNS), (b) core-shelled rubber (CSR) and (c) multi-walled carbon nanotubes (MWCNT). According to the literature reviewed, nanomodified epoxy adhesives exhibit enhanced mechanical properties of the nanocomposite. This can be credited to the synergistic effect of the nanoparticles with the epoxy adhesive. Studies have shown that the toughening mechanisms of nanosilica-modified epoxy improves the strength and modulus of elasticity of the nanocomposite. Epoxy adhesives modified with CSR exhibited improvement in fracture toughness and ductility, with slight reduction in modulus of elasticity and strength. MWCNT exhibited promising results by increasing strength, fracture toughness and modulus of elasticity of the nanocomposite despite having a few drawbacks such as poor dispersion and compatibility with epoxy.

3 Materials and Methods

Four types of tests, namely moisture ingress measurement, DSC tests, tensile test on dogbone specimens and three-point bending beam bond test, were conducted. All specimens were separated into five different groups depending on the epoxy adhesives that were utilized as the adhesives and CFRP matrix: (a) neat epoxy; (b) neat epoxy modified with 10% wt. commercial surface-modified nanosilica masterbatch (SMNS); (c) neat epoxy modified with 10% wt. commercial core-shell rubber masterbatch produced by a Manufacturer A (CSR Type-1); (d) neat epoxy modified with 10% wt. core-shell rubber commercial masterbatch produced by a Manufacturer B (CSR Type-2); and (e) neat epoxy modified with multi-walled carbon nanotube commercial masterbatch (MWCNT). To determine the effects of environmental degradation, following initial cure in ambient laboratory conditions (23°C at RH=50±10%) for 7 days, the five groups of samples were subjected the following environments: control—23 °C at RH 50±10% for 18 weeks; and accelerated conditioning protocol (ACP)—water immersion at 45±1°C for 18 weeks.

DSC tests were performed to measure the T_g and enthalpy relaxation of five different groups of epoxy adhesives under control and ACP. Mechanical properties of dogbone specimens of epoxy adhesives were determined by performing tensile test per ASTM D 638. Three-point bending beam bond test was utilized to determine the performance of bond between CFRP and concrete. ACI 440.9R-15 prescribes a conditioning temperature of 50°C (slightly lower than the T_g of most commercial epoxies) to avoid introducing the glass transition during the conditioning. In this study, a conditioning temperature of 45°C was used. This temperature was selected because the literature showed that the T_g of some the epoxy adhesives can drop to below 50°C during accelerated conditioning. [60].

Table 4: Test Matrix

Adhesive	Test Method	Exposure Condition Control/ACP	Exposure Time	Number of specimens in control and exposed group respectively
Neat Epoxy	1. DSC Test	Control at 23°C and RH 50±1%) + (Immersion at 45±1°C	18 weeks	3+3
	2. Tensile Test of Dogbone			7+7
	3. Three-Point Bending Test			5+5
SMNS	1. DSC Test	Control at 23°C and RH 50±1%) + (Immersion at 45±1°C	18 weeks	3+3
	2. Tensile Test of Dogbone			7+7
	3. Three-Point Bending Test			5+5
CSR Type-1	1. DSC Test	Control at 23°C and RH 50±1%) + (Immersion at 45±1°C	18 weeks	3+3
	2. Tensile Test of Dogbone			7+7
	4. Three-Point Bending Test			5+5

CSR Type-2	1. DSC Test	Control at 23°C and RH 50±1%) + (Immersion at 45±1°C	18 weeks	3+3
	2. Tensile Test of Dogbone			7+7
	3. Three-Point Bending Test			5+5
MWCNT	1. DSC Test	Control at 23°C and RH 50±1%) + (Immersion at 45±1°C	18 weeks	3+3
	2. Tensile Test of Dogbone			7+7
	3. Three-Point Bending Test			5+5

3.1 Materials

3.1.1 Epoxy adhesives. The base epoxy adhesive used in this study consisted of DGEBA monomer (EPON 826) with an epoxy equivalent weight (EEW) of 178-186 g/eq, and polyetheramine-based hardener (Jeffamine D-230) with amine hydrogen equivalent weight (AHEW) of 60 g/eq. The epoxy and hardener were mixed at a ratio of 100:33 by weight corresponding to the stoichiometric equivalence between the functional groups. Four different commercial nanoparticle-modified masterbatches were used to modify the properties of the base epoxy: (a) 40% wt. surface- modified-nano silica (SMNS) dispersed in DGEBA resin, (b) 25% wt. of 300 nm nominal particle diameter siloxane core-shell rubber nanoparticle (CSR Type1) dispersed in DGEBA resin (c) 40% wt. of 100 nm particle diameter siloxane core-shell rubber nanoparticle (CSR Type-2) dispersed in DGEBA resin and (d) MWCNT dispersed in DGEBA resin. Epoxy equivalent weight of the five different adhesives including the neat epoxy is presented in Table 5.

Table 5: Physical Properties of the epoxy adhesives

Adhesives/Masterbatch	Epoxy Equivalent Weight (EEW), g/eq.
EPON 826	180
SMNS	295
CSR Type-1	243
CSR Type-2	308
MWCNT	226

SMNS masterbatch contains surface-modified synthetic SiO₂ nanospheres of 20-nm average diameter with a narrow particle size distribution (maximum diameter 50 nm) dispersed in DGEBA. The masterbatch has high content of 40% silica. The masterbatch has a relatively low viscosity due to the agglomerate-free colloidal dispersion of the nanoparticles in the

DGEBA based epoxy resin. The surface modification process is kept proprietary by the manufacturer. The masterbatch was combined with the neat epoxy resin at 10% wt. loading of SMNS by the weight of epoxy (Table 6).

CSR Type-1 masterbatch contains nanoparticle which has a polysiloxane core and a polymethyl methacrylate (PMMA) shell dispersed at 25 wt% in a DGEBA resin. The nanoparticle nominal diameter is 300 nm. The masterbatch was combined with neat epoxy resin to obtain 10% wt. loading of CSR Type-1 by the weight of resin (Table 6).

CSR Type-2 masterbatch consists of 40 wt% CSR nanoparticles. The elastomeric component is a special silicone rubber that is dispersed in the DGEBA epoxy carrier as a very finely dispersed second phase. Per manufacturer's data sheet, the masterbatch contains 100-nm diameter silicone rubber CSR nanoparticles. The masterbatch was combined with neat epoxy resin to obtain 10% wt. loading of CSR Type-2 by the weight of resin (Table 6).

MWCNT/Epoxy based masterbatch has high concentration of MWCNT. The nanoparticle loading ratio in the masterbatch is kept proprietary by the manufacturer. The mixing ratio specified in Table 6 was recommended by the masterbatch manufacturer.

Table 6: The mixing ratio of the resin and masterbatch

Adhesive Categories	Mix Ratio (Epoxy: Masterbatch)
Epoxy: SMNS	3:1
Epoxy: CSR Type-1	3:2
Epoxy: CSR Type-2	3:1
Epoxy: MWCNT	4:1

3.1.2 Concrete. Concrete used to prepare beam specimens had a target design strength of 10,000 psi. For achieving high compressive strength, a low water to cementitious material ratio (w/cm) of 0.353 was maintained. The concrete mixture was composed of: river

sand, coarse aggregate with gradation curve #89, Portland Cement Type I/II and admixtures - air entrainer (Darex AEA), plasticizer and water reducer (Adva Cast 600 and WRDA 60). Coarse aggregate moisture content was determined as per ASTM C566, prior to mixing the concrete, to adjust the batch quantities. The moisture content of the coarse aggregate was found to be 8.60%. No pozzolans were included in the mix design. The mix design is shown in Table 7.

Ten 4 in x 8 in. concrete cylinders were fabricated. Average compressive strength was determined per ASTM C39. Average compressive strength at 7- and 28-day mark is reported in Table 8.

Table 7: Mix proportion of 10,000 psi small beam specimens

MATERIAL	SOURCE	WT. PER YD³ (LB)	SPECIFIC GRAVITY	VOL. PER YD³ (CF)	WT. PER BATCH (LB)
CEMENT	Holcim Cement Type I,II	840.0	3.15	4.27	93.3
WATER	Local	296.5	1.00	4.75	32.9
FINE AGG.	Natural River Sand	1181.2	2.460	7.69	131.2
COARSE AGG.	#89	1356.3	2.300	9.45	150.7
AIR ENTRAINER	Darex AEA	1.00 oz	1.02	0.001	3.3 ml
ADMIXTURE	WRDA 60	25.20 oz	1.15	0.026	82.8 ml
ADMIXTURE	Adva Cast 600	25.20 oz	1.08	0.026	82.8 ml
AIR (DESIGN)	Local	0.0		0.790	
TOTAL		3674.10		27.00	

Table 8: Average compressive strength of cylinders for design 10,000 psi strength.

Compressive Strengths (Cylinder Test)	Days	Cyl. #1	Cyl. #2	Cyl. #3	Cyl. #4	Cyl. #5	Average Compressive Strength (psi)
	7	7760	7570	7600	7830	7560	7664±110
	28	9770	10180	9960	10370	10062	10068±202

3.2 Specimen Preparation

3.2.1 Epoxy dogbone specimens. Fourteen Type V (ASTM D638) as shown in Figure 3.1 dogbone specimens of the five different groups of epoxy adhesives were prepared. Epoxy adhesive was injected with a syringe into a rubber mold as shown in Figure 3.2. The specimens were cured for 1 week at in standard laboratory conditions . After the curing period, dogbone specimens were removed from the mold and seven specimens from each group were subjected to control condition and ACP.

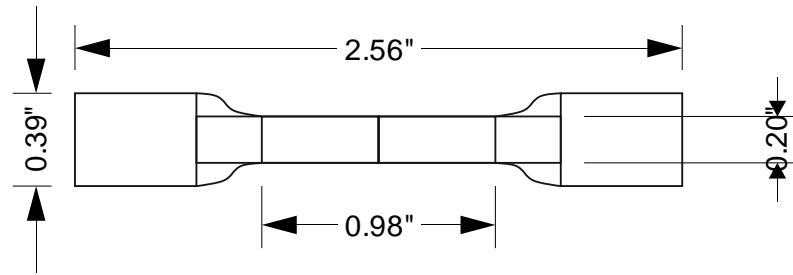


Figure 3.1: Dogbone specimen (Type V)




Figure 3.2: Epoxy injected into rubber mold

Neat epoxy preparation required mixing of epoxy resin with curing agent in a stoichiometric ratio. The mixture was stirred with a magnetic stirrer at 300 rpm for 20 minutes.

To prepare epoxy dogbone samples modified with SMNS, CSR Type-1 and CSR Type-2 nanoparticles the mixture of epoxy and masterbatch were stirred at 300 rpm at 80°C. The temperature was raised to reduce viscosity of the mixture and facilitate uniform dispersion of the nanoparticles during mixing. The hot mixture was allowed to cool down to ambient temperature by placing the mixture containing beaker in a water bath before curing agent (hardener) was added to it. A step by step procedure for preparing epoxy adhesives modified with a masterbatch is outlined in Table 9.

Table 9: Step by step preparation of epoxy adhesives

1. Acetone/ Isopropanol was used to clean the beaker, stirrer and spatula.	N/A
2. Weight of the empty beaker scale was measured using a scale (nearest two decimals).	

3. Epoxy (EPON 826) was poured into the beaker and measured.



4. The masterbatch containing nanoparticles was then poured into a beaker and heated on a hot plate to reduce viscosity. The temperature was maintained at 80°C.

N/A

5. Masterbatch was then added to the beaker containing neat epoxy. The mixture was then stirred on a hot plate at 300 rpm. A magnetic stirrer was added to the mixture.



6. After stirring the mixture for 10 minutes, the beaker was placed in a water bath and allowed to cool down.

N/A

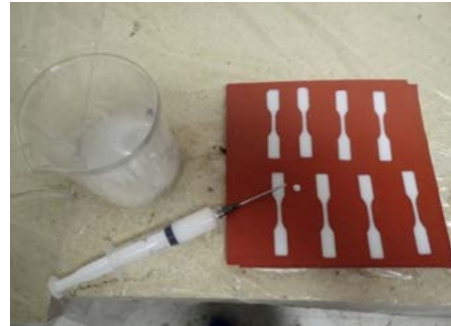
7. Hardener (JEFFAMINE D-230) was then poured into the beaker.



8. The final mixture containing epoxy, masterbatch and hardener was then mechanically stirred on the hot plate (without heating the mixture) for 10 minutes.



9. A syringe was used to inject the epoxy adhesive into the mold to form dogbone specimens.



Due to the well-known difficulties with dispersing MWCNT in epoxy, the mixing procedure was modified for the MWCNT/epoxy based masterbatch. The viscosity of the masterbatch was reduced by preheating it at 70°C-80°C. It was then mixed with neat epoxy resin. The mixture of epoxy and masterbatch was subjected to sonication for 20-30 minutes as shown in Figure 3.3. An amplitude of 30 μm was maintained until the temperature was raised to 70°C. Gradually, the amplitude was increased to 40 microns (μm) until the temperature reached

80°C. Following sonication, the MWCNT-modified resin was cooled down to ambient temperature by placing the container with the mixture in a water bath. Subsequently, hardener was added into the mixture for curing the modified epoxy sample. Finally, the mixture containing epoxy, masterbatch and hardener was subjected to high shear mixing with a mixer homogenizer at 2000 rpm for 20 minutes. After completing these steps, the nanomodified epoxy was poured into the dogbone mold.

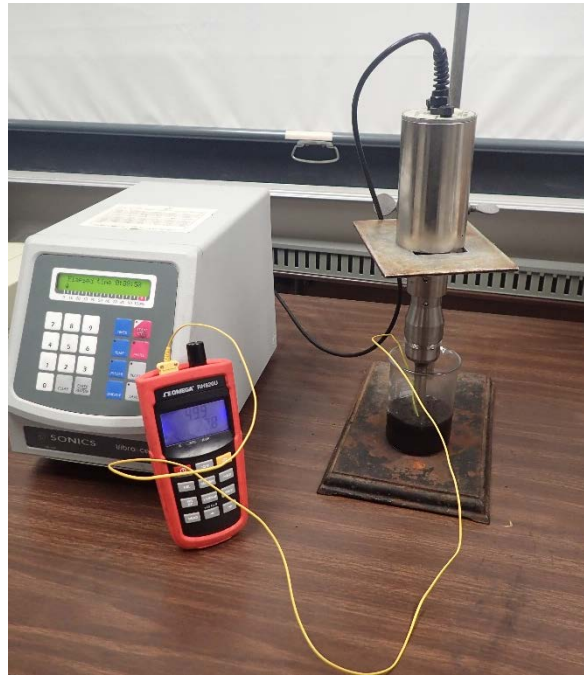


Figure 3.3: Dispersion of MWCNT based masterbatch epoxy by sonication

3.2.2 Differential scanning calorimetry (DSC). DSC samples were prepared by carefully polishing off small pieces of cured epoxy and placing them in the DSC pans. Aluminum pans of 30 μ L volume were used. Setaram DSC-131 was used to determine the T_g of five different adhesive groups subjected to control conditioning and ACP.

3.2.3 CFRP-reinforced beam specimens for bond performance

characterization. Fifty (50) 4x4x14 in. beam specimens were cast for three-point bending beam bond tests. Fine aggregate (sand) was oven-dried for 24 hours to minimize the absorbed moisture. Coarse aggregate was soaked in water for at least 24 hours to saturate at the time of mixing. Concrete was mixed in a portable mixer as shown in Figure 3.4. Coarse aggregate, sand and cement were added to the mixer first. Dry ingredients were mixed for 3-5 minutes before adding water to the mix. Water was poured gradually to achieve uniform dispersion. Admixtures were added into the mix to improve the workability. Slump was measured according to ASTM C143 and was found to be 5.5 inches. 3% air content of the concrete was determined as per ASTM C23.



Figure 3.4: Portable concrete mixer

Concrete was poured into aluminum-plywood forms as shown in Figure 3.5. The forms were coated with a form-release agent to facilitate beam removal and cleaning of the forms.

Concrete was poured half-way into the forms and vibrated for 30 seconds using a concrete vibrator (Figure 3.6).

Forms were fully filled and again vibrated for 30 seconds. Excessive concrete from the top surface was removed. The top surface was then leveled using a trowel. After filling the forms, concrete was allowed to harden for 24 hours before demolding. The beam samples were cured in a curing tank in lime solution according to ASTM C 31 for 28 days.

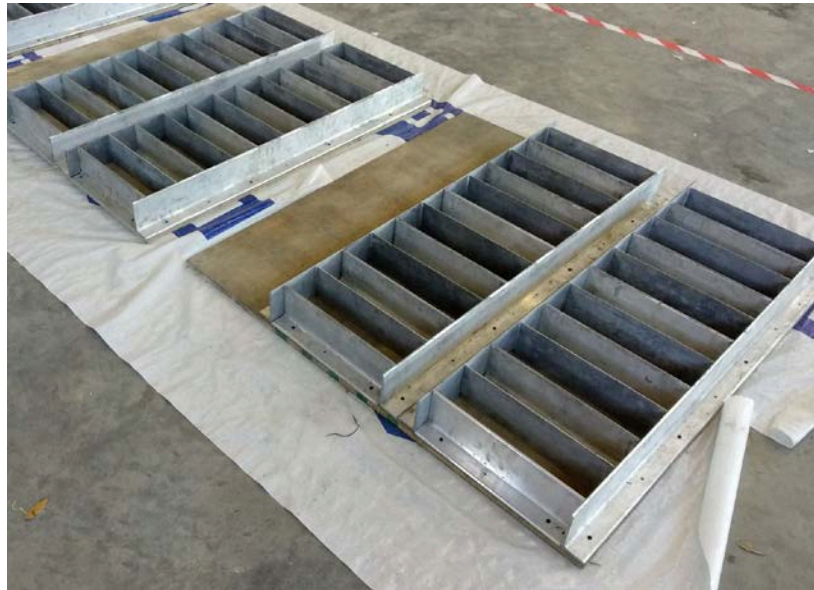


Figure 3.5: Aluminum-ply beam forms

Beam specimens were used to fabricate CFRP-reinforced beam specimens for bond performance characterization in three-point bending [61]. The specimen size of the concrete beam, load configuration, FRP geometry and material properties were selected according to ACI 440 [61]. Adequate cross-sectional area of externally bonded FRP was selected based on previous research studies [61]. In addition, a 2 inches' deep notch is introduced at the

midspan of the beam specimen to simulate crack and initiate debonding under Mode II loading condition (Figure 3.6).



Figure 3.6: Insertion of notch in the midspan of the small beam specimen

To achieve the optimum adhesion between the concrete surface and epoxy layer in surface bonded FRP reinforced beam specimen, the FRP placement area was subjected to needle scaling with a needle scaling gun (Figure 3.7)



Figure 3.7 : Needle scaling gun

Concrete beams were reinforced by applying CFRP strip across the notch tailored on the tension face of the beam as shown in Figure 3.8.



Figure 3.8: Insertion of CFRP on the tension surface of the beam specimens by wet layup process

3.3 Experimental Procedures

All experiments described in this section were performed for two groups of specimens, separated based on the conditioning environment they were subjected to: (1) control -23 °C at RH 50±10% for 18 weeks and (2) accelerated conditioning protocol (ACP) -water immersion at 45±1°C for 18 weeks.

3.3.1 Moisture ingress. Moisture ingress of ACP dogbone specimens was tracked throughout the exposure period. Initial weight of the dogbone specimens of the five groups of epoxy adhesives was measured using a weight scale (0.01g accuracy). The ACP dogbone specimens were placed in a zip-lock bag. Small holes were formed throughout the carrier bags to allow water pass through it. The carrier bags were then placed in the exposure tank. Once a week for 18 weeks (time of exposure) change in weight of the dogbone specimens were measured. Percentage increase in moisture content is calculated using the recorded initial weight and change in weight of the dogbone specimens, per following equation:

$$M_I = \frac{W_a}{W_i} \quad (1)$$

Where,

M_I = Average weight increase due to moisture ingress

W_a = Mass of absorbed water by the sample

W_i = Initial mass of the samples

3.3.2 Differential scanning calorimetry (DSC). DSC measurements were performed on three replicates for each of the test groups. The experiments were performed in Setaram DSC-131 at a heating rate of 10 °C/min with a starting temperature of 5°C and the end temperature at 100°C. Cooling period was set to 40 minutes. T_g of the epoxy adhesives are measured after the passage of first heating cycle.

3.3.3 Tensile tests. Five types of adhesives were used in the wet layup process (a) neat epoxy, (b) epoxy with 10 wt % SMNS and (c) epoxy with 10 wt% CSR Type-1, (d) epoxy with 10 wt% CSR Type-2 and (e) epoxy with MWCNT. The specified loading ratios correspond to the percentage weight of nanoparticles in a mixture of base epoxy resin and

masterbatch. Five specimens from each group were subjected to accelerated conditioning protocol (ACP) by water immersion under water at $45\pm 1^\circ\text{C}$ for 18 weeks (3024 hours).

Simultaneously, five specimens from each group were kept in the standard laboratory of RH $50\pm 10\%$ for 18 weeks (3024 hours).

Tensile tests were performed in a 100-kN MTS universal testing machine on epoxy dogbone samples according to ASTM D638. Tests were performed at a displacement controlled rate of 2 mm/min. VIC-2D Digital Image Correlation (DIC) system was used to obtain full-field displacement and strain measurements in the epoxy dogbone samples. Speckle pattern from a typical dogbone sample is shown in Figure 3.9

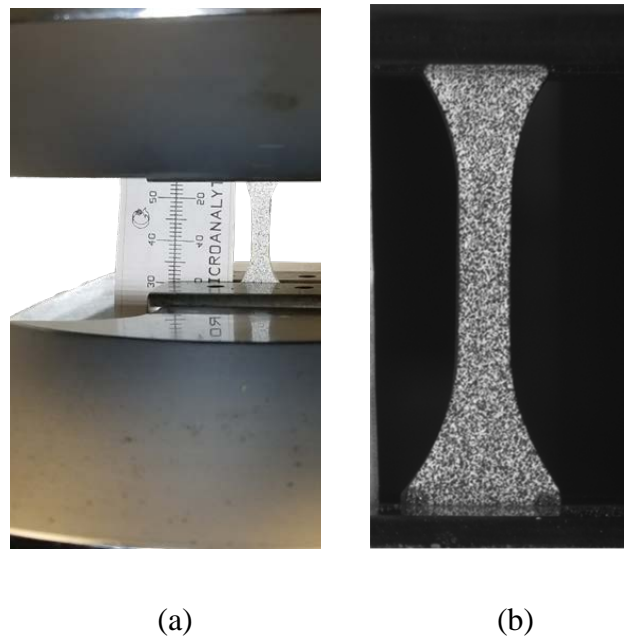


Figure 3.9: (a) Tensile test of dogbone specimen in mts; (b) Speckle pattern on a typical epoxy dogbone specimen

3.3.4 Three-point bending beam bond tests. The FRP-reinforced beam specimen as shown in Figure 3.10 were loaded in a 100-kN MTS universal testing machine. The span length was set at 12 inches. The simple supports were placed at previously marked positions

and the loading point was placed at the midspan above the notch . The test had been run at a displacement rate of 0.017 in/min. It took 3.5-4 minutes for each beam to fail in flexure by CFRP debonding.

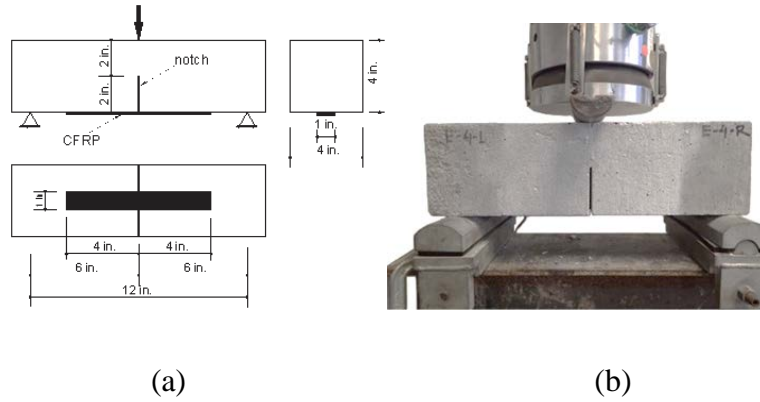


Figure 3.10: Three point bending test setup; (a) Small beam specimen specification; (b) Three-point bending test fixtures of notched beam specimens

4 Results and Discussion

4.1 Moisture Ingress

Average weight increase of all five groups of epoxy adhesive due to moisture ingress has been represented in Figure 4.1. Dogbone specimens of all five groups of epoxy adhesives under ACP experienced between approximately 1.5% and 2% weight increase due to water ingress. The data clearly showed that neat epoxy and epoxy modified with SMNS and CSR Type-1 have similar weight increase. After 18 weeks of exposure the increase in weight ranged between 1.5 wt%-1.75 wt%. However, MWCNT and CSR Type-2 exhibited higher moisture ingress compared to the other three types of adhesives. It was observed during specimen preparation that the viscosity of the epoxy modified with MWCNT and CSR Type-2 was significantly higher than that of the neat epoxy and epoxy modified with SMNS and CSR Type-1. High viscosity of the two adhesives is thought to have resulted in higher porosity of CSR Type-2 and MWCNT, which in turn induced higher moisture uptake.

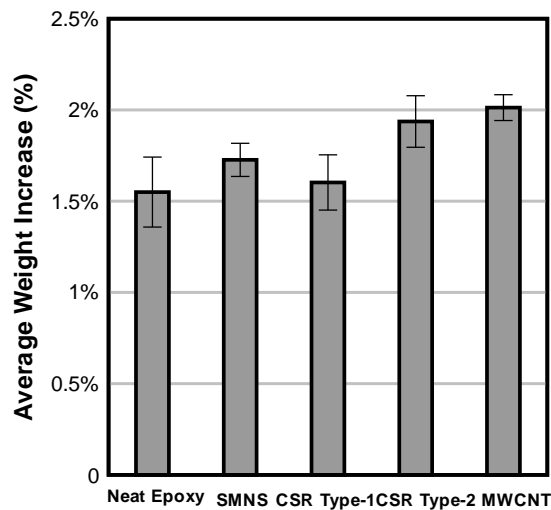


Figure 4.1: Moisture ingress of the epoxy adhesives

4.2 Glass Transition Temperature (T_g)

T_g of five different epoxy adhesives groups, measured for control and ACP are shown in Figure 4.2 (a). DSC curves of all five groups showed distinct glass transition region in all of the tested DSC sample as represented in Figure 4.2 (b). Based on the data, under control conditions addition of nanoparticles in the epoxy did not affect the T_g which indicates good compatibility between the base epoxy and nanoparticles.

Increase in T_g is observed in all the ACP groups over the control condition. The ACP group experienced an increase in T_g than the control group. This increase in T_g can be caused by post-cure at elevated temperature. Based on the data presented in Figure 4.2 (a) it appears that within the conditioning time post-cure was more dominant than the plasticizing effect in the ACP groups.

MWCNT and CSR Type -2 have higher moisture ingress compared to the other three groups (Figure 4.1); consequently, their T_g are lower than those of neat epoxy, SMNS, and CSR Type-1. It is likely that the effect of plasticization (indicated by higher moisture ingress) may have resulted in lower T_g of the abovementioned groups. Moreover – following ACP – neat epoxy specimens showed the highest average increase in T_g (21%) whereas MWCNT exhibited the lowest (14%) which, again, indicates that higher chain mobility caused by plasticization is characteristic of MWCNT and CSR Type-2 adhesives.

Enthalpy relaxation of five different epoxy adhesives groups, measured for control and ACP are shown in Figure 4.3. Due to post curing, loss in enthalpy relaxation occurs which is discussed earlier in chapter 2. Loss in enthalpy is highest in MWCNT, CSR Type-2 and neat epoxy. With aging at elevated temperature, crosslinking density increase which leads to an increase in T_g , while enthalpy relaxation is diminishing. Since, neat epoxy possesses highest

T_g , its change in enthalpy relaxation can be related to post-cure. Interestingly, MWCNT and CSR Type-2 exhibits significant loss in enthalpy relaxation despite possessing lower T_g in ACP than neat epoxy. This behavior can be related to moisture ingress of MWCNT and CSR Type-2 nanocomposite. Both MWCNT and CSR Type-2 have high moisture ingress. Due to high viscous nature of MWCNT and CSR Type-2, macro pores and voids may have been present within the molecular structure of the nanocomposites. Absorbed water may have occupied these macro pores and voids. Presence of water molecules may have participated in forming additional crosslinking with the polymeric chain at elevated temperature rather than inducing plasticizing effect. Presence of nanoparticle may also have played a positive role in post-cure in this two groups. However, the T_g values for SMNS and CSR Type-1 do not correlate with the loss in enthalpy. Despite having increased T_g , insignificant change in enthalpy is observed in SMNS and CSR Type-1 adhesive groups. Although research has been performed on changes in T_g and enthalpy in accelerated conditions for neat epoxy, studies on effect of nanoparticles in post-cure have yet to be explored. Further research is required to explain the abnormal behavior of nanomodified adhesive groups.

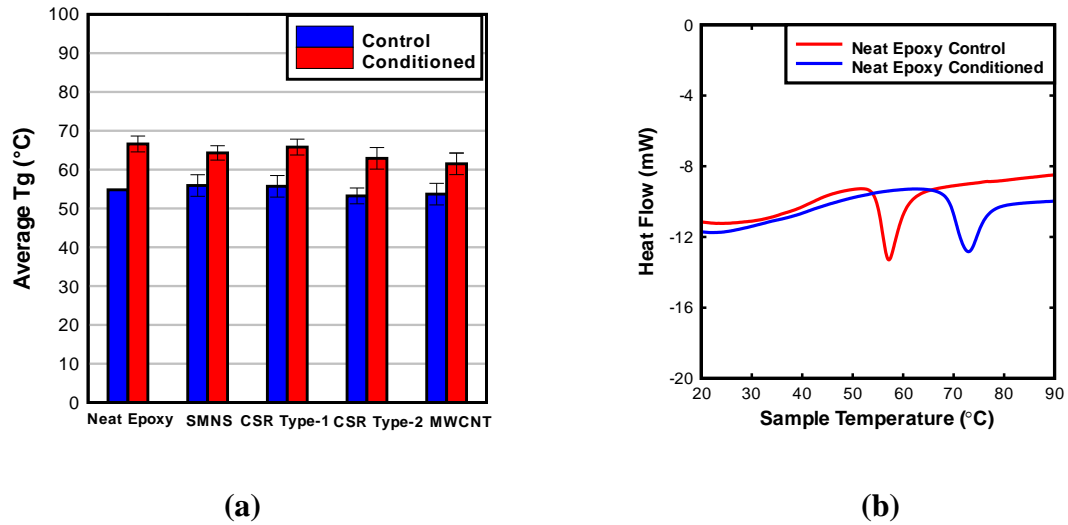


Figure 4.2: (a) Average T_g values of different sample; (b) Typical DSC curve of neat epoxy

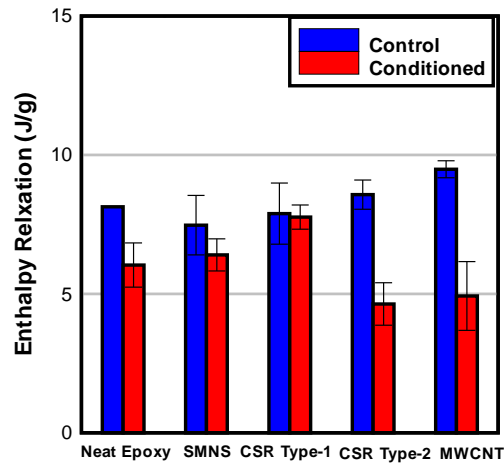


Figure 4.3: Enthalpy relaxation

4.3 Tensile Properties of Epoxy

Typical stress vs strain diagrams for five epoxy groups are shown in Figure 4.4 and Figure 4.5. All adhesives, with and exception of CSR Type-1 and CSR Type-2, showed elastic stress-strain behavior followed by a brittle failure. CSR-modified epoxy adhesive groups

exhibited ductile elongation prior to the failure. No significant difference in stress-strain behavior was observed between control and ACP groups, except that SMNS- and MWCNT-modified epoxies experienced a slight post-peak-stress plastic deformation following accelerated conditioning.

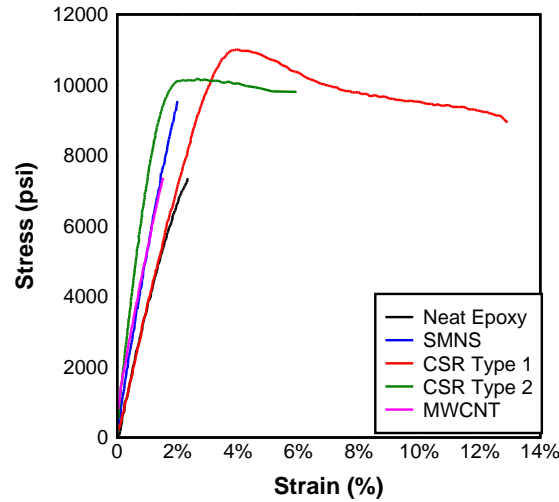


Figure 4.4: Typical stress vs strain curve of dogbone samples in control condition

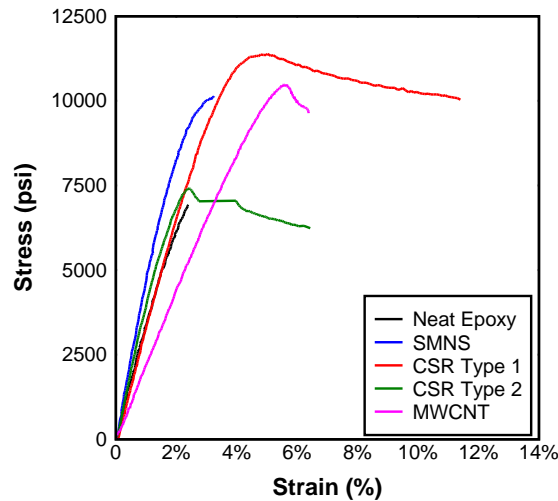


Figure 4.5: Typical stress vs strain curve of dogbone samples in acp

4.3.1 Strength. Comparison of strength among the different adhesive dogbone samples is shown in Figure 4.6. Change in mechanical properties was observed in epoxy adhesive groups with the addition of nanoparticles. Inherent toughening properties of CSR and nanosilica nanoparticles may have played a role in increasing the strength of the epoxy adhesive. Even though literature reports a decrease in strength in fully cured CSR-modified epoxy adhesives [50], it is thought that increase in strength of CSR-modified epoxy specimens in this study can be attributed to good compatibility and strong interaction between epoxy matrix and functional groups of CSR which ultimately results in a nanocomposite with superior mechanical properties to those of ambient-cured neat epoxy. When compared to neat epoxy, improvement is observed in strength for epoxy specimens modified with CSR Type-1 and CSR Type-2 by 33% and 25%. Epoxy samples modified with SMNS also exhibited increased strength of 16% more over the neat epoxy samples. However, epoxy samples modified with MWCNT nanoparticles showed a 5% decrease in strength. The reason behind the lack of improvement in strength of MWCNT-modified epoxy samples can be blamed on poor dispersion process of MWCNT in epoxy, and its relatively high viscosity which resulted in entrapped air bubbles (large defects) in epoxy dogbone specimens.

Following ACP, the neat epoxy experienced a 23% reduction in strength which can be explained by reduction in polymer network chain segment concentration caused by swelling [60]. Strength of nanomodified epoxy adhesive groups did not significantly change indicating that nanoparticles may be effective at offsetting the deteriorating effect of water.

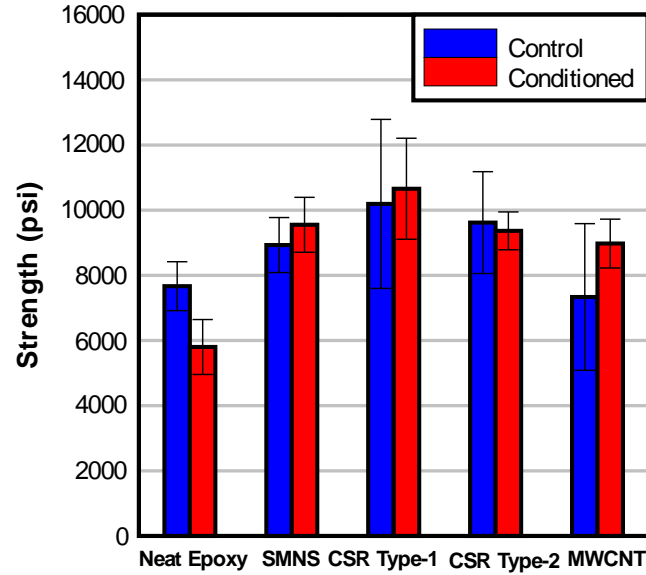


Figure 4.6: Strength of dogbone specimens in control and ACP

4.3.2 Elongation. Elongation of the epoxy adhesives improved when CSR nanoparticles were added, as shown in Figure 4.7. CSR Type-1 exhibited highest elongation at break of 12.43% which was an improvement by 400% over neat epoxy samples. Improvement in elongation is also evident in CSR Type-2. SMNS- and MWCNT-modified epoxy experienced a slight decrease in elongation when compared to neat epoxy likely due to the stiffening effect of SMNS and MWCNT on the epoxy which limits the deformation capacity.

Following ACP, no significant change in elongation was observed. Minor increase in average elongation were observed in SMNS-modified epoxy (47%), while MWCNT-modified epoxy showed a significant increase of 94%. Increase in elongation in SMNS and MWCNT groups can be accredited to post-peak-stress plastic deformation which was likely driven by plasticization of epoxy cross link network domains. CSR-modified epoxies show small changes in elongation between control and ACP groups that are well within the statistical error.

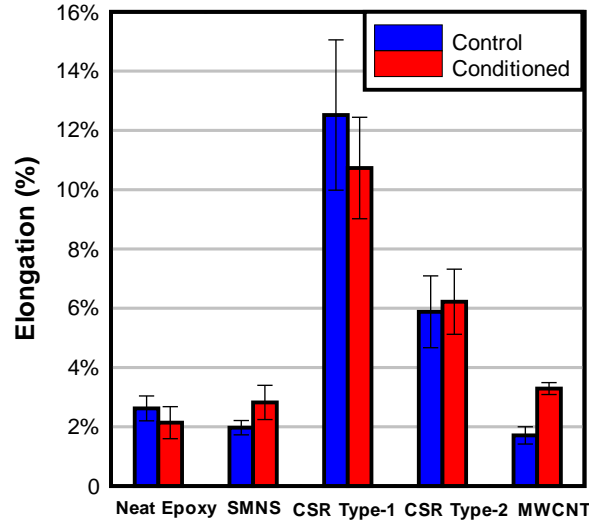


Figure 4.7: Elongation of dogbone specimens in control and acp

4.3.3 Modulus of elasticity. Moduli of elasticity for all five epoxy groups are shown in Figure 4.8. Under control conditions, the nanocomposites showed an increase in modulus of elasticity when compared to the neat epoxy group. While an increase in modulus of elasticity is typical for epoxy modified with SMNS and MWCNT [37], the literature reports a decrease in elastic moduli in CSR/epoxy nanocomposites mainly due to a relatively low modulus of the rubber particles [50]. Disagreement between the herein reported data and that found in the literature may be due to the curing conditions. In the literature, epoxy adhesives and their nanocomposites are subjected to staged cure which results in fully cured adhesives. On the contrary, all adhesives in this study were cured under ambient conditions which results incomplete cure with many unreacted functional groups. Uniformly dispersed CSR with reactive surface may have resulted in formation of bonds between unreacted epoxy functional groups and nanoparticles, causing an increase in the modulus of elasticity. After ACP, all epoxy groups except SMNS and MWCNT experienced a significant reduction in elastic modulus. The degradation in ACP samples is the most apparent in the CSR

modified epoxies. The modulus of elasticity (MOE) degraded by 20% and 22% respectively in CSR Type-1 and CSR Type-2 epoxy adhesives. Plasticization is deemed responsible for this behavior: increase the mobility of the molecular chains of the epoxy and free volume driven by moisture ingress leads to loss in modulus of elasticity [35].

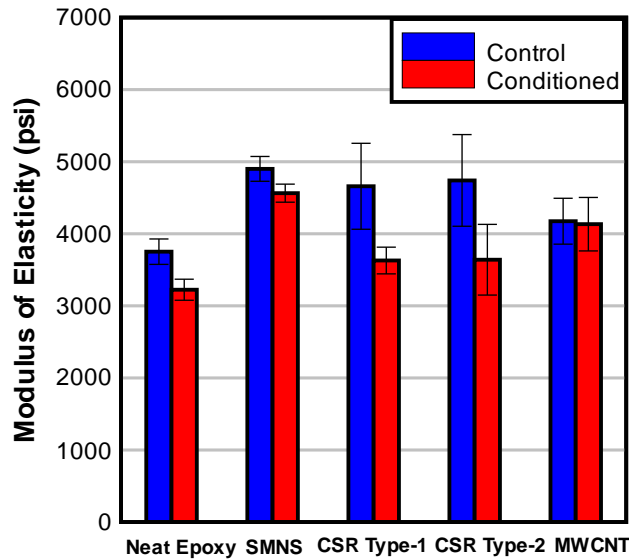


Figure 4.8: Modulus of elasticity of dogbone specimens in control and ACP

4.4 Three-point Bending Beam Bond Test Results

Typical load-displacement plots from the three-point bending tests are presented in Figure 4.9 and Figure 4.10. It is evident from the load-displacement plot that there were no apparent changes in stiffness as the specimens were loaded. Generally, changes in stiffness can be characterized by the occurrence of (a) microcracking near the interface, (b) formation of macrocracks, and (c) debonding of CFRP from the specimen [62].

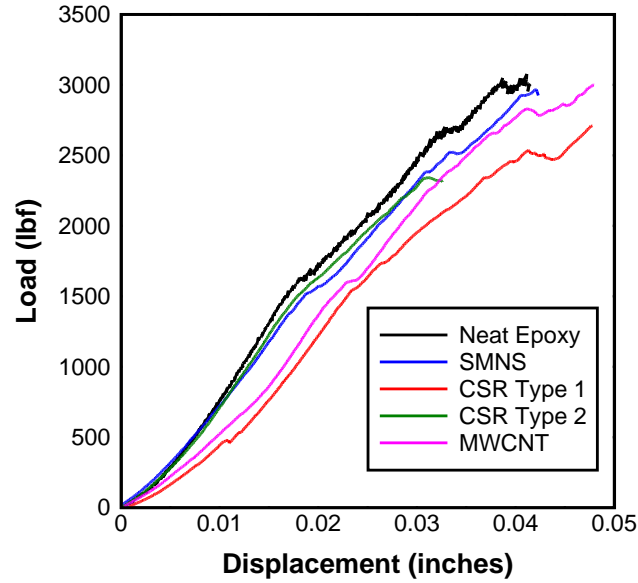


Figure 4.9: Load vs displacement curve for control specimens

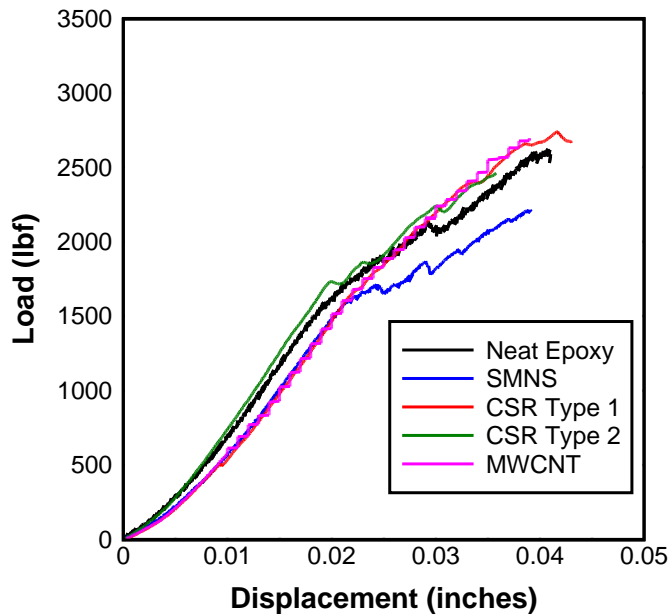


Figure 4.10: Load vs displacement curve for ACP specimens

Nanoparticle-modified epoxy adhesives do not significantly change FRP-concrete bond strength when compared to the neat epoxy. In control conditions, beam samples where neat epoxy was used as an adhesive showed highest strength compared to other group of

adhesives. Increased viscosity of nanomodified adhesives may have non-uniform wetting of beam surface and saturation of carbon fiber fabric with epoxy adhesives, and introduction of air bubbles along the interface. These artifacts could be responsible for slightly lower strength of samples with nanomodified adhesive joints. Despite having lower tensile strength properties compared to the nanomodified samples, neat epoxy provided highest beam strength in control conditions likely due to low viscosity which allows for proper wetting of the substrate.

Comparison between control and ACP beam specimens showed that CSR-modified adhesive joints experienced the least amount of degradation. Data presented in Figure 4.11 indicate that in ACP, the beam strength values for neat epoxy, SMNS, CSR Type-1 and MWCNT groups are similar. The beam strength of neat epoxy group degraded the most following ACP. As tensile tests on epoxy demonstrated, due to possible effects of plasticization and swelling, strength and stiffness of neat epoxy adhesive have deteriorated. The degradation of nanomodified epoxy adhesive groups was lower than the neat epoxy group. As a result, following accelerated conditioning beams bonded by neat epoxy adhesive had the highest degradation compared to other groups of adhesives.

Another possible explanation for the degradation of neat epoxy group could be the existence of an epoxide-rich region (uncured epoxy) along the interface between the substrate and the adhesive. Exposure to moisture facilitated plasticization effect in neat epoxy beam specimens. Presence of nanoparticles in other groups of epoxy adhesives possibly offset the negative effects of incomplete cure within the interphase region which resulted in lower degradation following ACP.

Lower beam strength exhibited by CSR Type-2 epoxy adhesive group can be explained by its potential lack of compatibility with carbon fiber fabric sizing resulting in incomplete saturation of the CFRP composite (Table 10). Additionally, evaluation of fractured adhesive joints (further described in the following section) revealed a significant amount of large voids within the interface which would result in lower bond strength (Table 10).

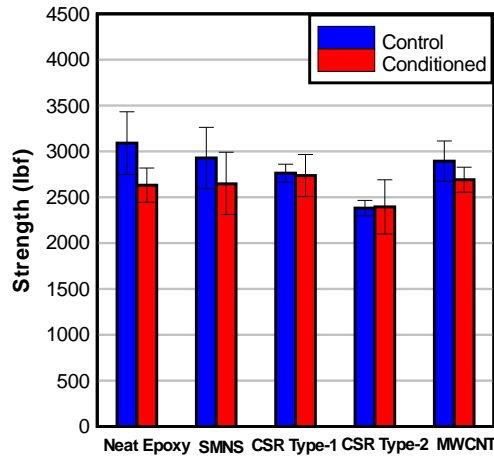


Figure 4.11: Strength of control and conditioned small beam specimens

To further evaluate the effect of nanomodified epoxy adhesives on bond degradation characteristics following ACP, bond strength retention was computed, per following equation:

$$R_b = \frac{ACP}{Q} \quad (2)$$

where,

R_b = Bond Strength Retention

ACP = strength of a sample subjected to ACP

Q = average control group strength

The purpose of the bond strength retention (R_b) is to characterize degradation in bond properties due to exposure in aggressive environments (as per ACI 440.2R-08). R_b is quantitatively expressed as Figure 4.12. The results clearly indicate the improvement in durability of bond in nanomodified epoxy over neat epoxy specimens. FRP-concrete bond toughened with CSR adhesives exhibits the maximum bond strength retention of approximately 100%, while the neat epoxy group demonstrates the lowest R_b value of approximately 0.85.

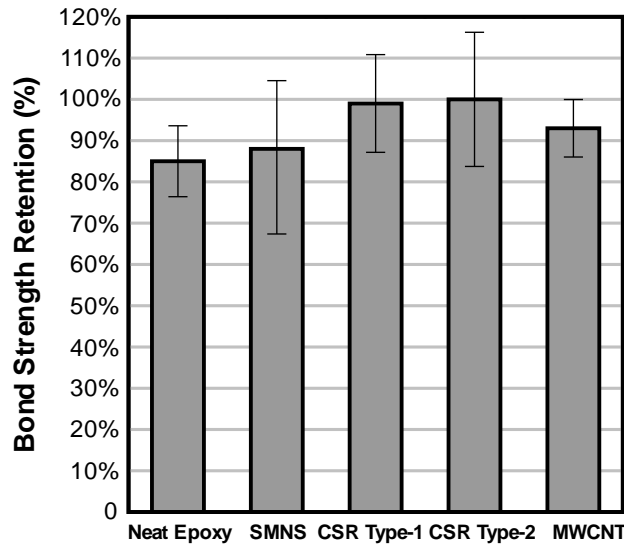


Figure 4.12: Bond strength retention

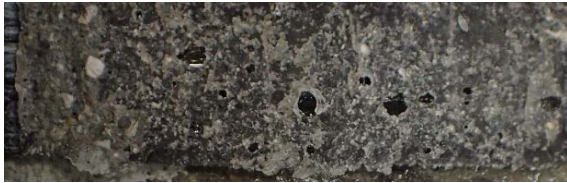


4.5 Failure Mode of CFRP-Concrete Adhesive Joints

The failed surfaces of the debonded CFRP and concrete substrate were analyzed by examining the debonded CFRP surfaces. Amount of concrete on the debonded CFRP surface can indicate the mode of failure in the specimens. The failure mode of control and ACP specimens are summarized in the Table 10.

All specimens experienced a mixture of cohesive and adhesive failure modes. This behavior was expected as high-strength concrete (10,000 psi) was intentionally used to maintain a failure surface along the interface so that interfacial degradation can be captured in the tests rather than durability of the concrete substrate.

Relative comparison in the amount of concrete “residue” on the failure surfaces did not reveal significant differences between different epoxy groups. Slight discrepancy can be observed in CSR Type-2 samples which showed an exceptionally high amount of entrapped air bubbles along the interface due to high viscosity of the adhesive and its possible incompatibility with the concrete substrate.

Table 10: Failure mode of control and ACP beam specimens

Type of Adhesive	Failure Image	Failure Mode
Neat Epoxy (Control)		Mixed (cohesive and adhesive)
Neat Epoxy (ACP)		Mixed (Cohesive and Adhesive)
SMNS (Control)		Mixed (Cohesive and Adhesive)
SMNS (ACP)		Mixed (cohesive and adhesive)



CSR Type-1
(Control)

Mixed (cohesive
and adhesive)



CSR Type-1 (ACP)

Mixed (cohesive
and adhesive)



CSR Type-2
(Control)

Mixed (cohesive
and adhesive)



CSR Type-2 (ACP)

Mixed (cohesive
and adhesive)



MWCNT
(Control)

Mixed (cohesive
and adhesive)



MWCNT (ACP)

Mixed (cohesive
and adhesive)



5 Summary and Conclusions

One of the most significant concerns with externally bonded FRP repairs is the potential occurrence of a sudden and brittle debonding failure. This concern becomes more prominent when FRP-concrete bond is subjected to environmental degradation induced by moisture. Ambient-cured low-viscosity epoxy adhesives based on Bisphenol A are most commonly utilized in the engineering practice to bond wet-layup FRP to the concrete surface. This research was conducted to understand if nanomodified epoxy adhesives can improve the durability of the adhesive joint between externally bonded FRP and concrete when subjected to hygrothermal conditioning. The presented research focused on the effects of Bisphenol A-based epoxy modified with commercial surface-modified nanosilica (SMNS), core-shell rubber (CSR) nanoparticles and multi-walled carbon nanotubes (MWCNT) particles on the improvement of mechanical properties of the nanomodified epoxy adhesives and strength and durability of FRP-concrete adhesively bonded joints.

To determine the effects of environmental degradation, following initial cure in ambient laboratory conditions (23°C at $\text{RH}=50\pm 10\%$) for 7 days, the five groups of samples were subjected the following conditioning protocols: control— 23°C at $\text{RH } 50\pm 10\%$ for 18 weeks; and accelerated—water immersion at $45\pm 1^{\circ}\text{C}$ for 18 weeks.

Experimental program consisted of: (a) moisture ingress measurement; (b) differential scanning calorimetry (DSC) tests to determine the glass transition temperature and enthalpy relaxation of the epoxy adhesives under control and ACP; (c) tensile tests on epoxy dogbone to characterize their mechanical properties; (d) three-point beam bond test on notched beam concrete samples reinforced with externally bonded CFRP; to determine the effect of

nanoparticle addition to epoxy on FRP-concrete bond strength and durability. Research findings are discussed below:

- CSR Type-2 and MWCNT have the maximum moisture uptake, 1.85% and 2 % respectively in 18 weeks' time. CSR type-2 and MWCNT had higher viscosity than the other groups of adhesives which may have resulted in higher porosity, which in turn induced higher moisture uptake.
- The control group experienced a T_g in the range from 53°C -55°C. The ACP group had T_g ranging from 61.5°C - 66.5°C. Increase of T_g following ACP can be accredited to post-curing of the epoxy adhesives.
- CSR- and SMNS-modified epoxy adhesives showed the largest improvement in strength. Compared to neat epoxy, improvement was observed in strength for epoxy specimens modified with CSR Type-1, CSR Type-2 and SMNS by 33%, 25% and 16%, respectively. Superior strength of CSR and SMNS than neat epoxy group can be accredited to good compatibility and strong interaction between epoxy matrix and functional groups present in CSR and SMNS nanoparticles. High viscosity of MWCNT-modified epoxy resulted in entrapped air bubbles (large defects) in epoxy dogbone samples leading to a 5% reduction in strength over neat epoxy. Poor dispersion of MWCNT in the epoxy may also be a reason for strength deterioration. Following ACP, the strength, of the neat epoxy reduced by 23
- CSR Type-1 exhibited highest elongation at break of 12.43% which was an improvement by 400% over neat epoxy group. SMNS and MWCNT exhibited lowest elongation of 2.0% and 1.7%, respectively. Following ACP, minor increase over control in average elongation were observed in SMNS-modified epoxy (42%), while

MWCNT-modified epoxy showed a significant increase of 92%. Increase in elongation in SMNS and MWCNT groups can be accredited to post-peak-stress plastic deformation possibly driven by plasticization of epoxy cross link network domains. CSR-modified epoxies showed small changes in elongation between control and ACP groups that were well within the statistical error. Following ACP, the elongation of the neat epoxy reduced by 22%.

- Under control conditions, SMNS and CSR modified nanocomposites showed an increase in modulus of elasticity of about 31% and 23% respectively over neat epoxy. Surprisingly, CSR-modified nanocomposites showed an increase in stiffness which disagreed with the literature findings. In the literature, however, epoxy adhesives and their nanocomposites are subjected to staged cure which results in fully cured adhesives. On the contrary, all adhesives in this study were cured under ambient conditions which results incomplete cure with many unreacted functional groups. It is thought that uniform dispersion along with high reactivity of CSR nanoparticles resulted in an increase of the modulus of elasticity.
- In control conditions, neat epoxy provided highest CFRP-concrete adhesive bond strength when compared to nanomodified adhesive groups. This occurred likely due to its low viscosity which allowed proper wetting of the substrate. In ACP, CSR-modified adhesive joints experienced practically no degradation. The bond strength of neat epoxy adhesive joints degraded most dramatically (15%) following ACP. CFRP-concrete bond toughened with CSR adhesives exhibits the maximum bond strength retention of approximately 100%.

- Post mortem inspection of CFRP and concrete surfaces showed that mixed failure mode dominated in control and ACP samples. This behavior was expected as high-strength concrete (10,000 psi) was intentionally used to maintain a failure surface along the interface so that interfacial degradation can be captured in the tests, rather than durability of the concrete substrate.

6 Future Work

The performed research raised many questions, which can be of interest for future work . In this research nanoparticle loading ratio of 10 wt% was evaluated. For further research, the ratio of nanoparticles to epoxy can be varied and their effect on bond durability should be assessed. Loading ratio of nanoparticles in the nanocomposite can play a vital role in enhancing the mechanical properties of the nanomodified epoxy. According to literature review ,lower loading ratio of MWCNT to epoxy (0.1-1.0 wt. %) provides the most enhanced mechanical properties. In this study, loading ratio of MWCNT was kept proprietary by the manufacturer. In the future work, loading ratio of MWCNT can be varied to understand its effect on enhancement of mechanical and adhesive properties of the adhesive. Similarly, loading ratio of other nanoparticles should also be varied.

Hybrid nanocomposite i.e. mixture of more than one nanoparticle in the nanocomposite shall be explored. Further research can be performed to understand the synergistic effect of different combinations of nanoparticles on the performance characteristics. As reported in the literature, addition of CSR and SMNS in epoxy can increase the ductility and the modulus of elasticity of the nanocomposite without decreasing the strength. Similarly, combination of other nanoparticles such as MWCNT and CSR or SMNS and MWCNT can be studied to determine the effect of such hybrid nanocomposites on durability of bond properties in FRP-concrete joints.

Moisture ingress adversely affects the modulus of elasticity of the epoxy and the chemical bonding between the epoxy and the concrete surface. Silane coupling agents should be explored to improve the chemical bond properties. Study on the synergistic effects of silane-

treated substrate and nanomodified adhesives on the adhesive bond behavior would be an important contribution to the body of knowledge.

In this research abnormal behavior regarding enthalpy relaxation of nanomodified epoxy adhesives (SMNS and CSR Type-1) were observed. The effect of nanoparticles on the thermal and hydrothermal aging can also be a topic for future work. Post-curing phenomenon in hydrothermal condition and its relation to enthalpy relaxation must be explored.

The exposure time can be prolonged or shortened and environmental factors such as UV, saltwater, freeze and thaw can be introduced to simulate realistic field conditions . Better understanding of the short- and long-term effect of moisture on bond can be achieved by developing conditioning protocols that effectively accelerate deterioration of FRP-concrete. Further studies can be done to form a correlation between debonding and growth of debonded areas with environmental and loading conditions.

7 References

- [1] L. Van Den Einde, L. Zhao, and F. Seible, "Use of FRP composites in civil structural applications," *Constr. Build. Mater.*, vol. 17, no. 6–7, pp. 389–403, 2003.
- [2] L. C. Hollaway, "A review of the present and future utilization of FRP composites in the civil infrastructure with reference to their important in-service properties," *Constr. Build. Mater.*, vol. 24, no. 12, pp. 2419–2445, 2010.
- [3] Karbhari, Vistasp M. "Fabrication, quality and service-life issues for composites in civil engineering." In *Durability of composites for civil structural applications*, pp. 13-30. 2007.
- [4] L. C. Bank, T. R. Gentry, B. P. Thompson, and J. S. Russell, "A model specification for FRP composites for civil engineering structures," *Constr. Build. Mater.*, vol. 17, no. 6–7, pp. 405–437, 2003.
- [5] L. C. Hollaway and M. Leeming, "Strengthening of reinforced concrete structures: Using externally-bonded FRP composites in structural and civil engineering". Elsevier, 1999.
- [6] L. C. Hollaway and J.-G. Teng, "Strengthening and rehabilitation of civil infrastructures using fibre-reinforced polymer (FRP) composites." Elsevier, 2008.
- [7] C. Carloni and K. V. Subramaniam, "Application of fracture mechanics to debonding of FRP from RC members", *ACI SP*, vol. 286, no. 10, pp. 1–20, 2012.
- [8] J. Tatar and H. R. Hamilton, "Comparison of laboratory and field environmental conditioning on FRP-concrete bond durability," *Constr. Build. Mater.*, vol. 122, pp. 525–536, 2016.
- [9] R. A. Hawileh, M. Z. Naser, and J. A. Abdalla, "Finite element simulation of reinforced concrete beams externally strengthened with short-length CFRP plates," *Compos. Part B Eng.*, vol. 45, no. 1, pp. 1722–1730, 2013.
- [10] H. Niu and Z. Wu, "Interfacial debonding mechanism influenced by flexural cracks in FRP-strengthened beams," *J. Struct. Eng.*, vol. 47, pp. 1277–1288, 2001.
- [11] Tatar, J., Blackburn, P., Weston, C., & Hamilton, H. R. "Direct shear adhesive bond test". In *Proc., 11th Int. Symp. of Fiber Reinforced Polymer for Reinforced Concrete Structures (FRPRCS-11)*. (2013)
- [12] N. Domun, H. Hadavinia, T. Zhang, T. Sainsbury, G. H. Liaghat, and S. Vahid, "Improving the fracture toughness and the strength of epoxy using nanomaterials—a review of the current status," *Nanoscale*, vol. 7, no. 23, pp. 10294–10329, 2015.

- [13] Frigione, Mariaenrica, and Mariateresa Lettieri. "Durability issues and challenges for material advancements in FRP employed in the construction industry." *Polymers* 10, no. 3 (2018): 247.
- [14] Tuakta, C., Buyukozturk O. (2010). "Deterioration of FRP/concrete bond system under variable moisture conditions quantified by fracture mechanics." *Composites Part B: Engineering* 42 (2): 145-154
- [15] Tatar, Jovan, and H. R. Hamilton. "Bond durability factor for externally bonded CFRP systems in concrete structures." *Journal of Composites for Construction* 20, no. 1 (2015): 04015027.
- [16] Xie, M., S. V. Hoa, and X. R. Xiao. "Bonding steel reinforced concrete with composites." *Journal of reinforced plastics and composites* 14, no. 9 (1995): 949-964.
- [17] F. Djouani, C. Connan, M. Delamar, M.M. Chehimi, K. Benzarti, "Cement paste–epoxy adhesive interactions", *Constr. Build. Mater.* 25 (2) (2011) 411–423.
- [18] Bicerano, Jozef. "Prediction of polymer properties". CRC Press, 2002.
- [19] S. Choi, "Study of hygrothermal effects and cure kinetics on the structure-property relations of epoxy-amine thermosets": Fundamental analysis and application. 2011.
- [20] Lettieri, M., Lionetto, F., Frigione, M., Prezzi, L., & Mascia, L. "Cold-cured epoxy-silica hybrids: Effects of large variation in specimen thickness on the evolution of the Tg and related properties". *Polymer Engineering & Science*, 51(2), 358-368, 2011.
- [21] Aiello, Maria A., Mariaenrica Frigione, and Domenico Acierno. "Effects of environmental conditions on performance of polymeric adhesives for restoration of concrete structures." *Journal of materials in civil engineering* 14.2 (2002): 185-189.
- [22] Ouyang, Zhenyu, and Baolin Wan. "An analytical model of FRP-concrete bond deterioration in moist environment." *Advances in Structural Engineering* 12.6 (2009): 761-769.
- [23] Corcione, Carola Esposito, Fabrizio Freuli, and Mariaenrica Frigione. "Cold-curing structural epoxy resins: analysis of the curing reaction as a function of curing time and thickness." *Materials* 7, no. 9 (2014): 6832-6842.
- [24] B. P. Blackburn, J. Tatar, E. P. Douglas, and H. R. Hamilton, "Effects of hygrothermal conditioning on epoxy adhesives used in FRP composites," *Constr. Build. Mater.*, vol. 96, pp. 679–689, 2015.
- [25] Frigione, Mariaenrica, et al. "Novel epoxy-silica hybrid adhesives for concrete and structural materials: Properties and durability issues." *Advanced Materials Research*. Vol. 687. Trans Tech Publications, 2013.

- [26] M. Frigione, M.A. Aiello, C. Naddeo, "Water effects on the bond strength of concrete/concrete adhesive joints." *Constr. Build. Mater.* 20 (2006) 957–970.
- [27] E. P. Douglas, H. R. Hamilton, J. C. Nino, A. Stewart, and J. Tatar, "Highly accelerated lifetime for externally applied bond critical fiber-reinforced polymer (FRP) infrastructure materials." Department of Materials, Science & Engineering University of Florida, 2014.
- [28] Sperling, Leslie H., "Introduction to physical polymer science." John Wiley & Sons, 2005.
- [29] Odegard, G. M., and A. Bandyopadhyay. "Physical aging of epoxy polymers and their composites." *Journal of Polymer Science Part B: Polymer Physics* 49, no. 24 (2011): 1695-1716.
- [30] Chiang, Martin YM, and Marta Fernandez-Garcia. "Relation of swelling and Tg depression to the apparent free volume of a particle-filled, epoxy-based adhesive." *Journal of Applied Polymer Science* 87, no. 9 (2003): 1436-1444.
- [31] Tatar, Jovan, Natassia R. Brenkus, Ghatu Subhash, Curtis R. Taylor, and H. R. Hamilton. "Characterization of adhesive interphase between epoxy and cement paste via Raman spectroscopy and mercury intrusion porosimetry." *Cement and Concrete Composites* 88 (2018): 187-199.
- [32] A. Stewart, "Study of Cement-Epoxy Interfaces, Accelerated Testing, and Surface Modification", Ph.D. Dissertation, University of Florida, Gainesville, FL, 2012.
- [33] E.H. Immergut, H.F. Mark, "Principles of plasticization. Plasticization and plasticizer processes", *Adv. Chem.* 48 (1965) 1–26.
- [34] J.M. Zhou, J.P. Lucas, "Hygrothermal effects of epoxy resin. Part I: The nature of water in epoxy. Part II: Variations of glass transition temperature", *Polymer* 40 (20) (1999) 5505–5522
- [35] T. D. Chang and J. O. Brittain, "Studies of epoxy resin systems: Part D: Fracture toughness of an epoxy resin: A study of the effect of crosslinking and sub-Tg aging," *Polymer Eng. Sci.*, vol. 22, no. 18, pp. 1228–1236, 1982.
- [36] Liu, Fang, Shiqiang Deng, and Jianing Zhang. "Mechanical Properties of Epoxy and Its Carbon Fiber Composites Modified by Nanoparticles." *Journal of Nanomaterials* 2017 (2017).
- [37] N. Domun, H. Hadavinia, T. Zhang, T. Sainsbury, G. H. Liaghat, and S. Vahid, "Improving the fracture toughness and the strength of epoxy using nanomaterials—a review of the current status," *Nanoscale*, vol. 7, no. 23, pp. 10294–10329, 2015.
- [38] S. Sprenger, "Epoxy resins modified with elastomers and surface-modified silica nanoparticles," *Polymer*, vol. 54, no. 18, pp. 4790–4797, 2013.

- [39] Liang, Y. L., and R. A. Pearson. "*Toughening mechanisms in epoxy–silica nanocomposites (ESNs)*." *Polymer* 50, no. 20 (2009): 4895-4905.
- [40] Chen, Chenggang, Ryan S. Justice, Dale W. Schaefer, and Jeffery W. Baur. "*Highly dispersed nanosilica–epoxy resins with enhanced mechanical properties*." *Polymer* 49, no. 17 (2008)
- [41] Zamanian, Milad, Mehrzad Mortezaei, Babak Salehnia, and J. E. Jam. "*Fracture toughness of epoxy polymer modified with nanosilica particles: Particle size effect*." *Engineering Fracture Mechanics* 97 (2013)
- [42] Chen, Li, Songgang Chai, Kai Liu, Nanying Ning, Jian Gao, Qianfa Liu, Feng Chen, and Qiang Fu. "*Enhanced epoxy/silica composites mechanical properties by introducing graphene oxide to the interface*." *ACS applied materials & interfaces* 4, no. 8 (2012)
- [43] Frigione, Mariaenrica, et al. "*Novel epoxy-silica hybrid adhesives for concrete and structural materials: Properties and durability issues*." *Advanced Materials Research*. Vol. 687. Trans Tech Publications, 2013.
- [44] Aiello, Maria A., Mariaenrica Frigione, and Domenico Acierno. "*Effects of environmental conditions on performance of polymeric adhesives for restoration of concrete structures*." *Journal of materials in civil engineering* 14.2 (2002): 185-189.
- [45] Lettieri, M., Lionetto, F., Frigione, M., Prezzi, L., & Mascia, L. "*Cold-cured epoxy-silica hybrids: Effects of large variation in specimen thickness on the evolution of the Tg and related properties*." *Polymer Engineering & Science*, 51(2), 358-368, 2011.
- [46] J. Chen, A. J. Kinloch, S. Sprenger, and A. C. Taylor, "*The mechanical properties and toughening mechanisms of an epoxy polymer modified with polysiloxane-based core-shell particles*," *Polymer*, vol. 54, no. 16, pp. 4276–4289, 2013.
- [47] H. R. Brown, J. A. Schneider, and T. L. Murphy, "*Experimental studies of the deformation mechanisms of core-shell rubber-modified diglycidyl ether of bisphenol-A epoxy at cryogenic temperatures*," *J. Compos. Mater.*, vol. 48, no. 11, pp. 1279–1296, 2014.
- [48] D. Carolan, A. Ivankovic, A. J. Kinloch, S. Sprenger, and A. C. Taylor, "*Toughening of epoxy-based hybrid nanocomposites*," *Polymer*, vol. 97, pp. 179–190, 2016.
- [49] A. J. Kinloch, D. Carolan, A. Ivankovic, S. Sprenger, and A. C. Taylor, "*Toughening of epoxy-based hybrid nanocomposites*."
- [50] Quan, Dong, and Alojz Ivankovic. "*Effect of core–shell rubber (CSR) nano-particles on mechanical properties and fracture toughness of an epoxy polymer*." *Polymer* 66 (2015): 16-28.

- [51] Quan, Dong, Neal Murphy, and Alojz Ivankovic. "Fracture behaviour of epoxy adhesive joints modified with core-shell rubber nanoparticles." *Engineering Fracture Mechanics* 182 (2017): 566-576.
- [52] Liu, Songlin, Xiaoshan Fan, and Chaobin He. "Improving the fracture toughness of epoxy with nanosilica-rubber core-shell nanoparticles." *Composites Science and Technology* 125 (2016): 132-140.30.
- [53] F. H. Gojny, M. H. Wichmann, B. Fiedler, and K. Schulte, "Influence of different carbon nanotubes on the mechanical properties of epoxy matrix composites—a comparative study," *Compos. Sci. Technol.*, vol. 65, no. 15–16, pp. 2300–2313, 2005.
- [54] T. H. Hsieh, A. J. Kinloch, A. C. Taylor, and I. A. Kinloch, "The effect of carbon nanotubes on the fracture toughness and fatigue performance of a thermosetting epoxy polymer," *J. Mater. Sci.*, vol. 46, no. 23, p. 7525, 2011.
- [55] Tang, Long-cheng, Hui Zhang, Jin-hua Han, Xiao-ping Wu, and Zhong Zhang. "Fracture mechanisms of epoxy filled with ozone functionalized multi-wall carbon nanotubes." *Composites Science and Technology* 72, no. 1 (2011): 7-13.
- [55] Kim, Myung-Gon, Jin-Bum Moon, and Chun-Gon Kim. "Effect of CNT functionalization on crack resistance of a carbon/epoxy composite at a cryogenic temperature." *Composites Part A: Applied Science and Manufacturing* 43, no. 9 (2012): 1620-1627.
- [56] Ayatollahi, M. R., S. Shadlou, and M. M. Shokrieh. "Fracture toughness of epoxy/multi-walled carbon nanotube nano-composites under bending and shear loading conditions." *Materials & Design* 32, no. 4 (2011): 2115-2124.
- [57] Ayatollahi, M. R., S. Shadlou, and M. M. Shokrieh. "Mixed mode brittle fracture in epoxy/multi-walled carbon nanotube nanocomposites." *Engineering Fracture Mechanics* 78, no. 14 (2011): 2620-2632.
- [58] Allaoui, Aïssa, Shuo Bai, Hui-Ming Cheng, and J. B. Bai. "Mechanical and electrical properties of a MWNT/epoxy composite." *Composites science and technology* 62, no. 15 (2002): 1993-1998.
- [59] Park, Soo-Jin, Hyo-Jin Jeong, and Changwoon Nah. "A study of oxyfluorination of multi-walled carbon nanotubes on mechanical interfacial properties of epoxy matrix nanocomposites." *Materials Science and Engineering: A* 385, no. 1-2 (2004): 13-16.
- [60] Savvilotidou, Maria, Anastasios P. Vassilopoulos, Mariaenrica Frigione, and Thomas Keller. "Development of physical and mechanical properties of a cold-curing structural adhesive in a wet bridge environment." *Construction and Building Materials* 144 (2017): 115-124.

- [61] A. Gartner, E. P. Douglas, C. W. Dolan, and H. R. Hamilton, "Small beam bond test method for CFRP composites applied to concrete," J. Compos. Constr., vol. 15, no. 1, pp. 52–61, 2010.
- [62] Au, Ching, and Oral Büyüköztürk. "Peel and shear fracture characterization of debonding in FRP plated concrete affected by moisture." *Journal of Composites for Construction* 10, no. 1 (2006): 35-47.
- [63] ASTM D3039/D3039M Standard Test Method for Tensile Properties of Polymer Matrix Composite Materials
- [64] ASTM D638 Standard Test Method for Tensile Properties of Plastics.
- [65] ASTM C143 / C143M - 15a Standard Test Method for Slump of Hydraulic-Cement Concrete
- [66] ASTM C231 / C231M - 17a Standard Test Method for Air Content of Freshly Mixed Concrete by the Pressure Method

Morshed, Syed. Bachelor of Civil Engineering, Islamic University of Technology, 2014;
Master of Science, University of Louisiana at Lafayette, Summer 2018
Major: Engineering, Civil Engineering concentration
Title of Thesis: Durability Properties of Nanomodified FRP-Concrete Adhesive Joints
Thesis Director: Dr. Jovan Tatar
Pages in Thesis: 85; Words in Abstract: 290

Abstract

Externally bonded fiber-reinforced polymer (FRP) composites represent a simple and economical solution for many repair and strengthening applications in concrete structures. However, the potential occurrence of sudden and brittle debonding failure in such repairs becomes prominent when FRP-concrete bond undergoes environmental degradation induced by moisture. Ambient-cured low-viscosity Bisphenol A epoxy adhesives are most commonly utilized in the engineering practice to bond wet-layup FRP to the concrete substrate. This study aims to elucidate the effects of Bisphenol A-based epoxy modified with commercial surface-modified nanosilica (SMNS), core-shell rubber (CSR) nanoparticles and multi-walled carbon nanotubes (MWCNT) on the improvement of mechanical properties of the epoxy adhesives, and strength and durability of FRP-concrete adhesively bonded joints. Moisture ingress in epoxy, DSC, tensile test on epoxy and three-point bending beam bond tests were performed. To determine the effects of environmental degradation, all specimens were subjected to the following environments: control—23 °C at RH 50±10% for 18 weeks; and accelerated conditioning protocol (ACP)—water immersion at 45±1 °C for 18 weeks. Improvement in mechanical properties were observed in dogbone specimens modified with nanoparticles without any reduction in glass transition temperature (T_g). In control conditions, nanomodified epoxy groups exhibited enhanced mechanical properties compared to the neat epoxy. Following ACP, strength, elongation and modulus of elasticity of neat epoxy deteriorated significantly, while no significant deterioration was observed in the

nanomodified group of adhesives. Among all the nanomodified adhesive groups CSR Type-1 showed most improvement in mechanical properties over neat epoxy group both in control condition and in ACP. CSR-modified adhesive joints experienced practically no degradation when subjected to ACP and showed the highest maximum bond strength retention of 100% among all the adhesive groups. The bond strength of neat epoxy adhesive joints degraded most dramatically (15%) following ACP.

Biographical Sketch

Syed Ahnaf Morshed was born on January 01, 1994, in Dhaka, Bangladesh. He attended the Gazipur Campus, Islamic University of Technology between 2010 and 2014 and received his Bachelor's in Civil Engineering degree in November 2014. He worked as a lecturer at a private university for two years before coming to the United States for higher studies. He joined the University of Louisiana at Lafayette, Department of Civil Engineering in January 2017 where he began to pursue his Master of Science in Civil Engineering.